



HAL
open science

Differential proteomic profiling of mitochondrial from , rat and human reveals distinct patterns of age-related oxidative changes

Karlfried Groebe, Frank Krause, Birgit Kunstmann, Hermann Unterluggauer,
Nicole H. Reifschneider, Christian Scheckhuber, Charturvedala Sastri, Werner
Stegmann, Wojciech Wozny, Gerhard P. Schwall, et al.

► To cite this version:

Karlfried Groebe, Frank Krause, Birgit Kunstmann, Hermann Unterluggauer, Nicole H. Reifschneider, et al.. Differential proteomic profiling of mitochondrial from , rat and human reveals distinct patterns of age-related oxidative changes. *Experimental Gerontology*, 2007, 42 (9), pp.887. 10.1016/j.exger.2007.07.001 . hal-00499024

HAL Id: hal-00499024

<https://hal.science/hal-00499024v1>

Submitted on 9 Jul 2010

HAL is a multi-disciplinary open access archive for the deposit and dissemination of scientific research documents, whether they are published or not. The documents may come from teaching and research institutions in France or abroad, or from public or private research centers.

L'archive ouverte pluridisciplinaire **HAL**, est destinée au dépôt et à la diffusion de documents scientifiques de niveau recherche, publiés ou non, émanant des établissements d'enseignement et de recherche français ou étrangers, des laboratoires publics ou privés.

Accepted Manuscript

Differential proteomic profiling of mitochondrial from *Podospora anserina*, rat and human reveals distinct patterns of age-related oxidative changes

Karlfried Groebe, Frank Krause, Birgit Kunstmann, Hermann Unterluggauer, Nicole H. Reifschneider, Christian Scheckhuber, Charturvedala Sastri, Werner Stegmann, Wojciech Wozny, Gerhard P. Schwall, Slobodan Poznanović, Norbert A. Dencher, Pidder Jansen-Dürr, Heinz D. Osiewacz, André Schrattenholz

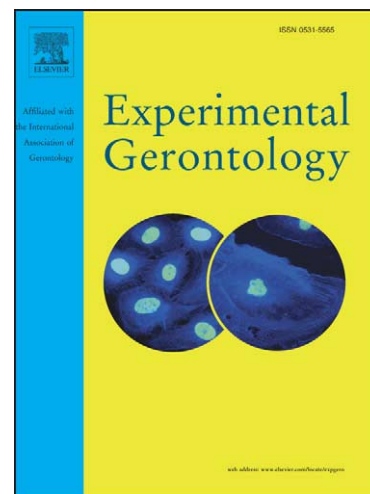
PII: S0531-5565(07)00147-7
DOI: [10.1016/j.exger.2007.07.001](https://doi.org/10.1016/j.exger.2007.07.001)
Reference: EXG 8367

To appear in: *Experimental Gerontology*

Received Date: 26 March 2007
Revised Date: 18 June 2007
Accepted Date: 6 July 2007

Please cite this article as: Groebe, K., Krause, F., Kunstmann, B., Unterluggauer, H., Reifschneider, N.H., Scheckhuber, C., Sastri, C., Stegmann, W., Wozny, W., Schwall, G.P., Poznanović, S., Dencher, N.A., Jansen-Dürr, P., Osiewacz, H.D., Schrattenholz, A., Differential proteomic profiling of mitochondrial from *Podospora anserina*, rat and human reveals distinct patterns of age-related oxidative changes, *Experimental Gerontology*(2007), doi: [10.1016/j.exger.2007.07.001](https://doi.org/10.1016/j.exger.2007.07.001)

This is a PDF file of an unedited manuscript that has been accepted for publication. As a service to our customers we are providing this early version of the manuscript. The manuscript will undergo copyediting, typesetting, and review of the resulting proof before it is published in its final form. Please note that during the production process errors may be discovered which could affect the content, and all legal disclaimers that apply to the journal pertain.



Differential proteomic profiling of mitochondrial from
Podospora anserina, rat and human reveals distinct
patterns of age-related oxidative changes

**Karlfried Groebe[†], Frank Krause[§], Birgit Kunstmann[‡], Hermann Unterluggauer[#],
Nicole H. Reifschneider[§], Christian Scheckhuber[‡], Charturvedala Sastri[†],
Werner Stegmann[†], Wojciech Wozny[†], Gerhard P. Schwall[†], Slobodan
Poznanović[†], Norbert A. Dencher[§], Pidder Jansen-Dürr[#], Heinz D. Osiewacz[‡]
and André Schratzenholz^{†*}**

[†] ProteoSys AG, Carl Zeiss Strasse 51, 55129 Mainz, Germany,

[§]Physical Biochemistry, Department of Chemistry, Darmstadt University of
Technology, Petersenstrasse 22, D-64287 Darmstadt, Germany.

[‡]Institute of Molecular Biosciences, Molecular Developmental Biology, Johann
Wolfgang Goethe-University, Marie-Curie-Str. 9, D-60439 Frankfurt, Germany.

[#]Institute for Biomedical Ageing Research, Austrian Academy of Sciences, Rennweg
10, A-6020 Innsbruck, Austria.

Acknowledgements:

This work was supported by EC FP6 Contract Nr. LSHM-CT-2004-512020;

(<http://www.mimage.uni-frankfurt.de>). This publication reflects only the authors'

views. The EC is not liable for any use that may be made of the information herein.

We thank S. Goto, H. Nakamoto, R. Takahashi (Toho University, Japan) and M.

Sugawa (Charité-Universitätsmedizin Berlin, Germany) for generously providing rat

brain tissue samples.

We thank Jennifer Schütz and Katja Biefang-Arndt for excellent technical assistance.

*Author to whom correspondance should be addressed:

Prof. Dr. André Schrattenholz, CSO

ProteoSys AG

55129 Mainz

Carl-Zeiss-Str. 51

Tel.: +49-6131-5019215

Fax: +49-6131-5019211

andre.schrattenholz@proteosys.com

Abstract

According to the 'free radical theory of ageing', reactive oxygen species are a key event during ageing of biological systems. Mitochondria are a major source of ROS and prominent targets for ROS-induced damage. Whereas mitochondrial DNA and membranes were shown to be oxidatively modified with ageing, mitochondrial protein oxidation is not well understood. The purpose of this study was an unbiased investigation of age-related changes in mitochondrial proteins and the molecular pathways by which ROS-induced protein oxidation may disturb cellular homeostasis. In a differential comparison of mitochondrial proteins from young and senescent strains of the fungal ageing model *Podospora anserina*, from brains of young (5 months) versus older rats (17 and 31 months), and human cells, with normal and chemically accelerated *in vitro* ageing, we found certain redundant posttranslationally modified isoforms of subunits of ATP synthase affected across all three species. These appear to represent general susceptible hot spot targets for oxidative chemical changes of proteins accumulating during ageing, and potentially initiating various age-related pathologies and processes. This type of modification is discussed using the example of SAM-dependent O-methyl transferase from *Podospora anserina* (PaMTH1), which surprisingly was found to be enriched in mitochondrial preparations of senescent cultures.

Introduction

The free radical theory of ageing (Harman, 1956) implicates molecular damage caused by reactive oxygen species (ROS) as a major cause of ageing processes in most if not all species. The mitochondrial theory of ageing linking mutations in mitochondrial DNA to the ageing process (Miquel et al., 1983; Miquel, 1991) has

subsequently found widespread support (for review see: Kowald, 2001; Wallace, 2001; Jacobs, 2003).

Age-related loss of mitochondrial functions has been demonstrated in various systems over the last several decades (Osiewacz and Hermanns, 1992; Osiewacz, 2002). In the filamentous fungus *Podospora anserina*, an extensively studied ageing model, mitochondrial DNA reorganisation is a hallmark of ageing of all wild-type strains (Esser et al., 1981; Stahl et al., 1978; Belcour et al., 1982; Belcour and Begel, 1980). Stabilization of mtDNA leads to increased lifespan. Some strains even appear to have acquired immortality (Koll et al., 1984; Schulte et al., 1988; Borghouts et al., 1997; Stumpferl et al., 2004). More recently, the impact of mitochondrial respiration on lifespan has been elaborated. A switch from a standard cyanide dependent respiration to an cyanide resistant, alternative pathway leads to a reduced generation of ROS and an increased lifespan (Schulte et al., 1988; Borghouts et al., 2001; Stumpferl et al., 2004; Gredilla et al., 2006; Dufour et al., 2000).

In the yeast *Saccharomyces cerevisiae*, the level of ROS production increases in naturally aged yeast mother cells (Laun et al., 2001). In *Caenorhabditis elegans* age-related mtDNA deletions were reported previously (Melov et al., 1995; Melov et al., 1995) and a systematic knock-down of mitochondrial genes via RNAi resulted in the generation of long-lived worm mutants (Lee et al., 2003). Using a mouse model, expressing a mutant mtDNA polymerase, it was shown recently that increased levels of point mutations and deletions of mtDNA can indeed cause a phenotype of reduced lifespan and premature onset of ageing-related phenotypes (Trifunovic et al., 2005; Kujoth et al., 2005). Whereas it is unlikely that increased oxidative stress results from mitochondrial dysfunction in these mouse models, it is currently unknown if the ageing phenotype is due to a disturbed energy metabolism or other causes, such as increased apoptosis (Kujoth et al., 2005).

Sporadic loss of mitochondrial function with ageing has also been observed in various rodent and mammalian tissues, and loss of function was correlated to the occurrence of mtDNA mutations, at least in some cases. In numerous non-reproductive tissues of many species, mitochondrial genes (like nuclear genes) accumulate mutations as the animals age (Vijg, 2000). The accumulation of mtDNA mutations can be explained either by a decreased degradation rate of damaged mitochondria or by a replication advantage of smaller mtDNA molecules (reviewed by Kowald et al., 2005).

The crucial role of mitochondria on intermediary metabolism and regulation is thus well established. Age-related mitochondrial dysfunction affects calcium signalling and downstream processes like apoptosis (Chan 2006). Irreversible lesions of mitochondrial genes or proteins have been shown to result in functional decline (Brookes et al. 2004; Brookes et al. 2002). Neuronal cells are especially vulnerable to mitochondrial damage due to excessive ATP demands of active synaptic regions. The crucial balance of ATP- and calcium homeostasis, explains the importance of mitochondria in many neurodegenerative diseases (Schrattenholz and Soskic 2006). Also, the critical role of ROS during ageing is broadly accepted (Singh 2006; Sanz et al. 2006; Kang and Hamasaki 2003; Osiewacz 2002). The gradual accumulation of irreversible oxidative modifications results in very specific patterns of redundant protein isoforms (Dencher et al. 2006), prompting this work as a systematic attempt to differentially quantitative conserved molecular patterns of age-related changes of mitochondrial proteins.

In the present study, we employed high resolution 2D-PAGE (Hunzinger et al. 2006), and three different ageing models: the filamentous fungus *P. anserina* with a clear mitochondrial etiology of ageing (Scheckhuber et al. 2007; Osiewacz 2002; Osiewacz

and Scheckhuber 2006), rats at three different ages, and different stages of a HUVEC (human umbilical vein endothelial cells) *in vitro* senescence model, applying both replicative senescence and premature (stress-induced) senescence.

Mitochondrial samples from these models were used to establish respective signatures of age-related differential proteins, which were subsequently analyzed for redundant posttranslational isoforms. It has recently been shown that there is a crucial relationship between resolution and differential quantification of proteins requiring isotopic labeling with a detection method providing sufficient dynamic range to enable statistical treatment of differences (Schrattenholz and Groebe, 2007). For relatively complex samples with redundant isoforms, high resolution 2D-PAGE has turned out to be a good compromise.

Despite the fact that the biological systems used in this study are from evolutionary far distant species, the focus on mitochondrial proteins resulted in some striking common mechanistic aspects. We find certain clusters of ROS-related modifications which occur in homologous mitochondrial (or mitochondria-associated) proteins across species.

On this background, systematic molecular profiling of age-related models, using proteomic and genomic platforms has gained considerable steam (Schieke et al. 2006; Weinreb et al. 2007; Vo and Palsson 2006), showing that proteomic signatures are directly correlated to activity-, cellular stress- and energy-dependent protein markers (Ding et al. 2006b; Johnson et al. 2006; Forner et al. 2006).

Proteins and pathways identified as being affected by age- and ROS -dependent posttranslational modifications in our study are discussed with a focus on two

representative cases, ATP synthase (Arrell et al. 2006; Krause et al. 2005) and SAM-dependent O-methyl transferase (Averbeck et al. 2000).

Materials and Methods

Isolation of crude mitochondrial fractions from rat brain

Left brains of 5-, 17-, and 31-month-old male rats (F344/DuCrj, purchased from Charles River Japan) were obtained from the animal facility at Toho University (Japan). The *ad libitum* fed rats had a mean life span of 29 months (Takahashi and Goto, 1987). Brain tissue was frozen in liquid nitrogen immediately upon dissection and stored at -80 °C for 1 – 5 years until isolation of mitochondria. Long-term storage of bovine heart mitochondria under these conditions for at least 16 months did not affect the yield of OXPHOS-supercomplexes (Krause et al. 2005). Rat brain mitochondria were isolated as gentle as possible (crude mitochondrial fraction) as described by Krause et al. (2005). A half brain was homogenized by a 2 ml tight-fit glass-teflon homogenizer (clearance 45–65 µm) with nine strokes (1100 rpm) after addition of 4 volumes of homogenization buffer (350 mM sucrose, 5 mM HEPES–NaOH, 1 mM EDTA, and 0.5 mM protease-inhibitor Pefabloc SC, pH 7.4) to 1 volume of tissue and the homogenate was centrifuged at 1300g (4 °C, 3 min). The pellet was extracted twice with each 2 and 1 ml homogenization buffer, respectively, and 1500g centrifugation. Thereafter, the combined supernatants were centrifuged with 17,000g (10 min, 4 °C). The crude mitochondrial pellet was washed once and resuspended in 320 mM sucrose, 0.5 mM Pefabloc SC. Finally, all isolated mitochondria were frozen as aliquots (5 – 7 mg/ml protein) in liquid nitrogen and stored at -80 °C.

Isolation of mitochondrial proteins from *P. anserina*

Mitochondria were isolated from juvenile and senescent *P. anserina* cultures, respectively, according to a previously published protocol (Gredilla et al. 2006) with the following modifications. Crude mitochondria were isolated by differential centrifugation for 35 minutes at 15.000 g and 4°C. The mitochondrial pellet was resuspended in 1 ml of mitochondria isolation buffer (10 mM Tris, 1mM EDTA, 0.33 M sucrose, pH7.5) and layered on a 20-50 % discontinuous sucrose gradient. After centrifugation for 1 hour at 100.000 g in a swing-out bucket rotor (TH641) the mitochondria were banding between the 50 and the 36 % sucrose step. Approximately 30 ml mitochondrial isolation buffer without BSA were added to the collected mitochondria fraction and centrifuged for 15 min at 15.000 g at 4°C. Special care was taken to ensure standardized processing times in individual preparations of mitochondria. Following this strategy three pairs of mitochondria (protein content: ~1 mg) from juvenile and senescent wild-type strain were isolated (analytical scale). In addition, one pair of mitochondria from juvenile and senescent cultures was prepared at a preparative scale of approximately 4 mg total mitochondrial protein. The differential pooling scheme for proteomic analyses is shown together with results (Figure 2).

HUVEC cell culture:

Endothelial cells were isolated from human umbilical veins as described by (Jaffe et al. 1973) and cultured in Endothelial Cell Basal Medium (Cambrex BioScience, Verviers) supplemented with EGM Singlequots (Cambrex BioScience, Verviers), containing 0.1% hEGF, 0.1% hydrocortisone, 0.1% GA-1000, 0.4% BBE and 2% FBS. The cells were subcultured by trypsinization with trypsin-EDTA (Gibco Life Technologies, Vienna, Austria), seeded on cell culture dishes coated with 0.2% gelatine and grown in an atmosphere of 5% CO₂ at 37°C. Cells were passaged at a

ratio of 1:5 in regular intervals. At later passages, the splitting ratio was reduced to 1:3 and 1:2, respectively. Cells were passaged such that the monolayers never exceeded 70–80% confluency. PDL were estimated using the following equation: $n = (\log_{10} F - \log_{10} I)/3.01$ (where n is the population doublings, F ; number of cells at the end of one passage, and I ; number of cells that were seeded at the beginning of one passage). After roughly 65 population doublings, the cells reached growth arrest, corresponding to 90-95% SA- β -Galactosidase positive cells.

Tertiary butylhydroperoxide (tBHP) treatment (stress induced senescence) = chemical ageing:

Young cells were treated on five consecutive days with 50 μ M tBHP (Fluka) for one hour each. After treatment, cells were washed twice with PBS and cultivation continued in standard EGM until the next tBHP-treatment. Following the last stress, the cells were cultivated for 24 hours in EGM and harvested for preparation of crude mitochondrial extracts.

Isolation of Mitochondria from HUVEC

Preparation of crude mitochondrial extracts was done according to the general guidelines (Rickwood and Hayes 1984) by differential centrifugation. All buffers and devices for extraction were ice-cooled. HUVEC of different replicative age were grown on 145mm culture dishes, rinsed twice with ice-cold PBS, scraped off the dishes and resuspended in 5ml homogenisation buffer [10mM HEPES pH 7.4; 1.1mM EDTA; 0.5%BSA and the antioxidant mixture SCAVEGR [(available at www.brainBitsLLC.com; see (Brewer et al. 2006)] and collected by centrifugation at 500g for 2min. The resulting pellet was again resuspended in Homogenisation buffer and homogenized in an iced - glass Teflon potter at 500rpm. After immediate addition

of Sucrose (0.25 molar) the suspension was centrifuged two times for 10min with 1500g and the resulting mitochondria-enriched supernatants collected. In a final step this crude mitochondria were pelleted by centrifugation at 13700g for 10min, washed twice in resuspension buffer [10mM HEPES pH 7.4; 0.25M Sucrose; 1.1mM EDTA plus protease inhibitor cocktail (Complete Mini EDTA free tablets from Roche)] and snap frozen in liquid nitrogen. Protein concentration of samples was determined by Bradford assay.

High resolution IEF/SDS-PAGE: 2D-PAGE was performed by 54 cm daisy chain serial IPG-IEF as described (Hunzinger et al. 2006). Briefly, shock-frozen samples were thawed at 25 °C and dissolved in 8M Urea, 4% CHAPS, 0.1M Tris pH 7.4. The volume was adjusted to 20 µL if necessary, followed by incubation of the sample at room temperature for 30 min with shaking at 1000 rpm in a Thermomixer comfort (Eppendorf). The samples were centrifuged for 5 min at 12000 rcf and 25 °C, and the soluble extracts were collected by removing the supernatant.

Experimental design, quantification and protein identification: The experimental strategy for obtaining statistically significant results about differential protein abundances using ProteoTope inverse replicate gels was performed as described previously (Poznanovic et al. 2005;Schrattenholz and Groebe 2007;Neubauer et al. 2006). In brief, protein iodination reactions with either ^{125}I or ^{131}I were conducted with identical chemical iodine concentrations. Less than 1 mg of protein from each radiolabelled sample were mixed and separated by 2-D PAGE high resolution daisy chains covering a pH range of 4–9. A high sensitivity radio imaging technique was applied to discriminate between ^{125}I and ^{131}I signals in one 2-D PAGE gel and to generate a quantitative multicolour differential display of proteins from separate

samples labelled with different iodine isotopes. For each pair of samples, reverse replicate gels were prepared, i.e., the labels (^{125}I and ^{131}I) used on sample 1 and sample 2 were inverted. Depending on the respective biological system, a total of two to five individual samples per age group entered the study, so the statistical evaluation was based on four to ten data points in each age group.

Depending on the number of age groups in each biological system, different pooling schemes were applied as shown in Figure 2. In the case of 2 groups (juvenile vs. senescent; Figure 2a), young subjects were individually compared to the pool of all old subjects, and old subjects were individually compared to the pool of all young subjects. In the case of three or more age groups (Figure 2b), each subject from each age group was individually compared to a common pool of all subjects.

Abundance ratios of one group vs. another are obtained by dividing the abundance ratios of the respective groups vs. the common pool. The former layout has the advantage that the measured differences in protein abundance are larger (than in comparisons involving a common pool) and that it provides a *direct* comparison between the conditions of interest (whereas in comparisons via a common pool each comparison between two age groups depends on *two* individual measurements). As its major disadvantage, the former pooling scheme can only be applied to two samples.

Gel image analysis was performed using the Pic/Greg software package by the Fraunhofer Gesellschaft in Sankt Augustin

(http://www.fit.fraunhofer.de/projekte/greg/index_en.xml) as described previously

(Hunzinger et al. 2006). Spot quantification and statistical identification of differential spots was performed as described (Schrattenholz and Groebe 2007). In brief, protein

spots were included if spot volume was at least $1 \cdot 10^{10}$ (in units used by Greg) and background intensity was at least four times less than spot intensity. All spots were checked manually using the Pic program and accepted or rejected depending on their actual appearance. Individual protein spot abundance ratios for the different conditions were statistically analyzed by t-tests and only those spots meeting significance criteria were subjected to MALDI-TOF peptide mass fingerprinting, as published before (Vogt et al. 2005). To this end, selected spots were excised from the gel by a picking robot (ProPick, Genomic Solutions Ltd, Huntingdon, UK) and proteins in gel pieces were trypsin digested using a ProGestrobot (Genomic Solutions Ltd, Huntingdon, UK). A ProMS-robot (Genomic Solutions Ltd, Huntingdon, UK) was used to apply samples for MALDI-TOF mass spectrometry onto an anchor target (Bruker, Bremen, Germany). Mass spectra of peptide ions were obtained using an Ultraflex MALDI time-of-flight (TOF) mass spectrometer (Bruker, Bremen, Germany) in reflector mode within a mass range from m/z 800 to 4000. The MS spectra were calibrated and annotated automatically. The resulting peptide mass fingerprints were searched against the non redundant NCBI Protein Sequence Database using Mascot Server software v. 1.8. (Matrix Science, London, UK).

Results

Mitochondria were isolated by differential centrifugation from cell pellets obtained by collecting cultured human endothelial cells, *P. anserina* cultures and by homogenization of freshly prepared rat brains. The experimental procedures for mitochondrial isolation except that for *P. anserina* mitochondria were purified by sucrose density centrifugation whereas mitochondria from rats and cell cultures were isolated by differential centrifugation. The subsequent proteome analysis was the same for the three species, providing both mitochondria of comparable quality and

statistically significant results. In the case of HUVEC, additional samples were collected after exposure to mild oxidative stress, known to induce a phenotype of premature senescence (Unterluggauer et al., 2003). As shown in Figure 1, by representative false colour images of radioactive spot intensities on high resolution 2D gels (pH range 4-9) of mitochondrial preparations of the three species investigated (rat brain, upper panel, *P. anserina* in the middle and human cells in the lower part), there are overall quite distinct patterns of protein expression and a variety of age-related differential spots. Despite the differences of patterns, replicates were highly reproducible and identified proteins were homologous in some cases or relating to similar pathway in other cases. The experimental strategy for obtaining statistically significant results about differential protein abundances using ProteoTope inverse replicate gels and identifying them by tracer-controlled preparative gels was performed as described previously (Poznanovic et al. 2005; Schrattenholz and Groebe 2007; Neubauer et al. 2006).

Several hundreds of such gels have been differentially quantified in inverse duplicates for each of the following conditions and according to the pooling scheme shown in Figure 2: Thus, excluding contributions from variations of individual protein patterns, mitochondrial preparations of juvenile and senescent *P. anserina* cultures were compared (Table S1). Then mitochondrial brain proteins of young rats (5 months) were compared against those of middle-aged (17 months; Table S2) and old rats (31 months, Table S3). Also a comparison of the middle-aged group against the old group was included (Table S4). In a further set of experiments human cells were compared in the same way, results from the comparison of young and senescent HUVEC cells are shown in Table S5 and corresponding results from a model of chemically accelerated ageing (young and tBHP-treated HUVEC cells as described in Unterluggauer et al. 2003) are compiled in Table S6.

In Table 1, we have summarized examples of age-related proteins with redundant isoforms, i.e. MALDI-TOF based identifications of the same amino acid backbone (and GeneBank accession #), but with slight differences in spectra and 2D gel positions. We listed all redundant isoforms found for SAM-dependent O-methyltransferase (SAM-OMT, PaMTH1), ATP-synthase F1 complex and reticulocalbin. These differences on the background of a single amino acid sequence always indicate posttranslational modifications, and they can be expected to be age-related because of our particular experimental paradigms.

Proceeding from identifying such multiple redundant isoforms, we see that differential abundances of related spot pairs are quite distinct: As shown in Figure 3 and Table 1, there are subunit isoforms of ATP synthase with relatively large differential amplitudes (e.g. spots 1192 and 1555 from *P. anserina*), as well as others with relatively subtle differences. This is due to the fact, that underlying posttranslational modifications are associated with distinct domains of ATP synthase subunits; whereas other parts of the protein remain unaffected. As will be shown below, there are indications from detailed inspection of mass spectra that ROS-related oxidative chemical reactions are responsible on the molecular level.

In both age-dependently differential isoforms of SAM-OMT shown in Figure 4 and Table 1, we found N-formylkynurenine-modifications (by typical characteristic mass increments of 4, 16 and 32 at respective peptides) (Bienvenut et al. 2002; Simat and Steinhart 1998). The specific oxidized sites are at tryptophanes W 35, 37 und 56. and abundances of this oxidative modification are different between juvenile and senescent *P. anserina* cultures: W 35 and 37 are more oxidized in senescent strains (~50% N-formylkynurenine in senescent vs. ~25% N-formylkynurenine in juvenile cells).

Taken together, our data show that some common targets for protein modification as a result of ageing can be identified in the three model systems applied in the current study. Moreover, at least one particular oxidative modification, the dioxygenation of aromatic tryptophane residues to N-formyl-kynurenine occurs in an age-dependent manner in one of the models investigated. This relatively stable type of carbonylation by ROS will serve as a marker of age-related events in the ongoing study.

Discussion:

Alterations in mitochondrial structure or function have been implicated in a variety of human diseases, ageing and longevity for quite some time. Since the initial reports of age-related mtDNA reorganization in *P. anserina* in the late 1970's and early 1980's (Stahl et al., 1978; Cummings et al., 1979) (Kück et al., 1981; Osiewacz and Esser, 1984) and complete sequencing of the human mitochondrial genome in 1981, enormous progress has been made in understanding the the relationship between mitochondrial energy metabolism and ageing (Gillardon 2006;Schrattenholz and Soskic 2006;Marin-Garcia et al. 2006;Lesnefsky and Hoppel 2006;Ruiz-Romero et al. 2006). So far 800-1200 mt-proteins have been described (Reinders et al. 2006; Alonso et al. 2005;Bailey et al. 2005) and organized in corresponding public databases (Prokisch et al. 2006;Basu et al. 2006). This also includes mtDNA information, with ROS-related mutations and subsequent consequences on the protein level (Rottenberg 2006; Capri et al. 2006).

Obviously mitochondrial genes and even more so, proteins can have different biological roles at different ages, and the constant generation of ROS accumulates to age-dependent decline of function. Recent data from invertebrate (Dufour et al., 2000; Gredilla et al., 2006; Borghouts et al., 2002) and animal models for ageing (Trifunovic et al., 2005) as well as from human cell cultures {Stoeckl et al., 2006} tend

to suggest that, besides mitochondrial ROS production, other consequences of mitochondrial dysfunction, e.g. a reduction of ATP levels (Stoeckl et al., 2006) (Zwerschke et al., 2003; Wang et al., 2003; Stoeckl et al., 2007 in press), may contribute to cellular and organismic ageing. Nevertheless, the available data still suggest a key role for ROS-induced damage in ageing. To address a potential role of ROS-induced protein damage in an unbiased way, we used a proteomics approach in the current study. Concerning the chemical nature of oxidative modifications, we focussed on the differential analysis of ROS-related posttranslational modifications, like N-formyl-kynurenine (Hunzinger et al. 2006) in redundant protein spots, like the ones demonstrated for putative SAM-dependent O-methyltransferase (PaMTH1), which was age-dependently carbonylated at distinct W-residues in *P. anserina* is homologous to catecholamine O-methyltransferase (COMT) in higher organisms (Averbeck et al. 2000) which in mammals is part of dopamine metabolism and has been shown to play key role in a variety of age-related human neurological disorders. By finding a COMT-homologue as being associated with mitochondria and modified by ROS-and age-related molecular changes, we support recent reports about impairments in mitochondrial functions contribute to the pathogenesis of Morbus Parkinson (Eriksen et al. 2005; Ding et al. 2006a; Jin et al. 2005). For the first time, we have indications linking dopamine-related metabolism and mitochondrial processes and it would be interesting to compare our proteomic results to age-dependent mtDNA deletions causing functional impairment in aged human substantia nigra neurons and Parkinson disease (Bender et al. 2006; Kraysberg et al. 2006). Moreover, the identification of of PaMTH1 in the sucrose density purified mitochondrial fraction was surprising because the link of such a protein to mitochondria is new. In the initial identification this protein was found to increase in quantity during the ageing of *P. anserina* in total protein extracts.

Finally, we found ATP synthase affected by age-dependent processes across all species investigated. This is in line with recent reports about specific protein oxidation and protein expression in aged rat brain, conditions of neuronal stress or under caloric restriction, where ATP synthase F1 β and α subunits were consistently among markers found (Poon et al. 2006c; Poon et al. 2006a; Sultana et al. 2006; Poon et al. 2005; Poon et al. 2006b; Kim et al. 2006). Our findings establish ATP synthase firmly as one of the prime mitochondrial targets of age-related molecular changes. Since the protein was uniformly affected in all models investigated in this study, we assume here a conserved mechanism of ageing represented by a “hot spot” of accumulating ROS-related damage. This finding suggests that functional inactivation of ATPase by posttranslational modification may directly contribute to the loss of intracellular ATP levels found in senescent human cells (Wang et al., 2003; Zwerschke et al., 2003; Stoeckl et al., 2006; 2007)(and possibly in aged tissue as well).

Some of the differential proteins found in the HUVEC model and others in rat and *P. anserina* point to downstream consequences of ROS-related damage of ATP synthase on dopamine- and proteasome-related pathways. Moreover we found indications that the intrinsic mitochondrial pathway of apoptosis regulated via the mitochondrial transition pore (Deniaud et al. 2006; Schrattenholz and Soskic 2006; Soskic et al. 2007) is involved. The mitochondrial transition in turn regulates mitochondrial autophagy observed in ageing (Cavallini et al. 2007; Donati et al. 2006; Terman and Brunk 2006). ROS-effects from oxidative phosphorylation and ATP synthase upon reductive defence mechanisms and apoptosis (Piec et al. 2005; Soti and Csermely 2006; Deocaris et al. 2006) are in line with our finding of age-dependence of cyclophilin D, a part of the mitochondrial permeability transition pore

and support the free radical theory of ageing (Poon et al. 2006c;Poon et al. 2006a;Sultana et al. 2006;Poon et al. 2005;Poon et al. 2006b;Kim et al. 2006).

Last but not least, our results from mitochondria preparations with HUVEC add to the increasing evidence that mitochondrial proteins interact intimately with the endoplasmic reticulum, Golgi and other organelles (Dolman et al. 2005; McMahon et al. 2006), and that this localisational dynamics is moving mitochondrial proteins (or their posttranslational derivatives!) to a variety of cytosolic and membrane compartments including even the outer plasma membrane. We hope that our data can contribute to providing a novel and more comprehensive understanding of the molecular consequences of energy metabolism on ageing, longevity and cellular stress management. It is noteworthy that the best-studied example of this class of proteins is the F_1F_0 ATP synthase (Yonally and Capaldi 2006), which we were able to profile in considerable detail in this study.

Figure legends

Figure 1: Representative images of high resolution 2D gels of mitochondrial preparations from the three ageing models: The IEF-range of these high resolution gels employing 54 cm serial IPG's, was from 4-9, and the range of apparent molecular masses was from 200 to 10 kD.

Dual isotope labelling allowed differential quantification of proteins from two samples in one experiment: In the upper part the differential display of the pattern of one particular 31 month old rat against the pattern of the pool of all rats is shown. In the middle, mitochondria from senescent *P. anserina* were compared against a pooled preparation from juvenile cells and in the bottom part, mitochondrial material from senescent HUVEC against pooled material from juvenile HUVEC.

In each case, the load was 10 µg of mitochondrial proteins labelled with I-125 and I-131, respectively. The radioactive quantities of differential spots in inverse replicates of such experiments provided absolute pattern control and served as basis for statistical analysis of age-dependent molecular changes. These experiments were meant for differential and quantitative pattern analysis and statistics only, the bulk of material was subsequently used for mass spectrometry-based identification of age-dependent mitochondrial proteins from tracer-controlled and silver-stained preparative gels as described previously (Hunzinger et al. 2006).

Figure 2: Schematic cartoon showing the design of the pooling paradigms for differentially comparing age-related changes of protein expression. Key is quantitative pattern control and unequivocal identification of differential proteins by radioactive dual-isotope labelling of senescent and juvenile mitochondrial preparations. The two radioisotopes are colour-coded as orange (^{131}I) and blue (^{125}I); and individual sample pairs (which were subsequently analyzed in single high

resolution 2D gels) are depicted on top of each other (note the always complementary isotopes). For each sample pair, inverse replicates were analyzed (highlighted with an additional box in Figure 2a and subsequently by vertical bars), providing independent measurements of protein concentrations, applicable to statistical analysis. The inserts show results for individual proteins.

In the paradigm for comparing two conditions only, individual samples (e.g. Ju1-Ju4 or Se1-Se4) of one condition were always compared to the pool of the other condition, and vice versa, as shown in Figure 2a. Thus, individual freak contributions could reliably be eliminated. In the case of three or more conditions of a model (e.g. 5, 17 and 31 months old rats), a common pool of all of these conditions was differentially compared to individual samples (Figure 2b). The differences between conditions are calculated as the total of the differences of the individual conditions with respect to the common pool (Figure 2b). The latter methodology could also be applied if there are only two conditions; it would, however, lead to smaller absolute differences in spot volumes and hence larger relative errors. Both approaches give similar results.

The statistical robustness originated from the application of these schemes to four independent paradigms using models from three species (*P. anserina*, *R. norvegicus*, *Homo sapiens*).

Figure 3: Dual false colour images of all redundant protein isoforms and subunits found for ATP synthase in four age-related models from three species: Names of specific subunits are shown beneath respective redundant spots in 2D-gels. Each one of them represents different molecular entities and the examples, which are labeled by spot numbers (see also Table 1) include isoforms with highly significant differences in concentration, as well as others with not much of a change. The larger

the difference, the clearer the false colour red-blue difference; the pI range of IPG's where the respective spots were found is indicated. Taken together, the underlying biophysical basis is posttranslational modifications, which are expected to yield direct information of hot spots of ROS-related damage. The structural information relating certain domains which are affected and potentially interacting proteins could translate to functional implications and a novel understanding of age-related cascades of dysfunction.

Figure 4: Putative SAM-dependent O-methyltransferase (PaMTH1) from *P. anserina*, which is homologous to catecholamine-O-methyltransferase (COMT) in higher organisms, is differentially oxidized and carbonylated in an age-dependent manner.

In Figure 4A, the dual false colour images from inverse replicates of a differential and quantitative comparison of senescent and juvenile cells in each one 2D gel are shown (each 10 μ g), the differences between the two conditions are consistent and statistically significant (for details see Table S1). In Figure 4B, a similar frame of the corresponding tracer-controlled and silver stained preparative 2D gel is shown (250 μ g loaded). The trace amounts of I-125 labelled samples comigrating with the silver stained spots 6 and 7, again helped to control patterns in complex 2D-gel images, as described previously.

In Figure 4C, details of the MALDI-TOF identification are given; both spots 6 and 7 come to the same protein identity. The more detailed MS-based investigation revealed an age-dependent difference of N-formylkynurenine modifications of tryptophane residues W-35 and W-37 of the protein.

References

1. Alonso J., Rodriguez J.M., Baena-Lopez L.A., Santaren J.F. (2005) Characterization of the *Drosophila melanogaster* mitochondrial proteome. *J Proteome Res* 4:1636-1645
2. Arrell D.K., Elliott S.T., Kane L.A., Guo Y., Ko Y.H., Pedersen P.L., Robinson J., Murata M., Murphy A.M., Marban E., Van Eyk J.E. (2006) Proteomic analysis of pharmacological preconditioning: novel protein targets converge to mitochondrial metabolism pathways. *Circ Res* 99:706-714
3. Averbeck N.B., Jensen O.N., Mann M., Schagger H., Osiewacz H.D. (2000) Identification and characterization of PaMTH1, a putative O-methyltransferase accumulating during senescence of *Podospora anserina* cultures. *Curr Genet* 37:200-208
4. Bailey S.M., Landar A., Darley-Usmar V. (2005) Mitochondrial proteomics in free radical research. *Free Radic Biol Med* 38:175-188
5. Barros, M. H., Bandy, B., Tahara, E. B. and Kowaltowski, A. J. (2004) Higher respiratory activity decreases mitochondrial reactive oxygen release and increases life span in *Saccharomyces cerevisiae*. *J Biol Chem* 279, 49883-49888.
6. Basu S., Bremer E., Zhou C., Bogenhagen D.F. (2006) MiGenes: a searchable interspecies database of mitochondrial proteins curated using gene ontology annotation. *Bioinformatics* 22:485-492

7. Belcour, L. and Begel, O. (1980) Life-span and Senescence in *Podospora anserina*: Effect of Mitochondrial Genes and Functions. *J. Gen. Microbiol.* *119*, 505-515.
8. Belcour, L., Begel, O., Keller, A.M., and Vierny-Jamet, C. (1982) Does Senescence in *Podospora anserina* Result from Instability of the Mitochondrial Genome? *Biology of the Cell* *43*, 11-21
9. Bender A., Krishnan K.J., Morris C.M., Taylor G.A., Reeve A.K., Perry R.H., Jaros E., Hersheson J.S., Betts J., Klopstock T., Taylor R.W., Turnbull D.M. (2006) High levels of mitochondrial DNA deletions in substantia nigra neurons in ageing and Parkinson disease. *Nat Genet* *38*, 515-517
10. Bienvenut W.V., Deon C., Pasquarello C., Campbell J.M., Sanchez J.C., Vestal M.L., Hochstrasser D.F. (2002) Matrix-assisted laser desorption/ionization-tandem mass spectrometry with high resolution and sensitivity for identification and characterization of proteins. *Proteomics* *2*, 868-876
11. Borghouts, C., Kimpel, E., and Osiewacz, H.D. (1997). Mitochondrial DNA rearrangements of *Podospora anserina* are under the control of the nuclear gene *grisea*. *Proc. Natl. Acad. Sci. U. S. A* *94*, 10768-10773.
12. Borghouts, C., Scheckhuber, C.Q., Werner, A., and Osiewacz, H.D. (2002). Respiration, copper availability and SOD activity in *P. anserina* strains with different lifespan. *Biogerontology* *3*, 143-153.
13. Borghouts, C., Werner, A., Elthon, T., and Osiewacz, H.D. (2001). Copper-modulated gene expression and senescence in the filamentous fungus *Podospora anserina*. *Mol. Cell Biol.* *21*, 390-399.

14. Brewer J., Benghuzzi H., Tucci M. (2006) Effects of thymoquinone, lycopene, and selenomethione in the presence of estrogen on the viability of SiHa cells in vitro. *Biomed Sci Instrum* 42, 37-41
15. Brookes P.S., Pinner A., Ramachandran A., Coward L., Barnes S., Kim H., Darley-Usmar V.M. (2002) High throughput two-dimensional blue-native electrophoresis: a tool for functional proteomics of mitochondria and signaling complexes. *Proteomics* 2, 969-977
16. Brookes P.S., Yoon Y., Robotham J.L., Anders M.W., Sheu S.S. (2004) Calcium, ATP, and ROS: a mitochondrial love-hate triangle. *Am J Physiol Cell Physiol* 287, C817-C833
17. Capri M., Salvioli S., Sevini F., Valensin S., Celani L., Monti D., Pawelec G., De B.G., Gonos E.S., Franceschi C. (2006) The genetics of human longevity. *Ann N Y Acad Sci* 1067, 252-263
18. Cavallini G., Donati A., Taddei M., Bergamini E. (2007) Evidence for Selective Mitochondrial Autophagy and Failure in Ageing. *Autophagy* 3, 26-27
19. Chan D.C. (2006) Mitochondria: dynamic organelles in disease, ageing, and development. *Cell* 125, 1241-1252
20. Cummings, D.J., Belcour, L., and Grandchamp, C. (1979) Mitochondrial DNA from *Podospora anserina* and the occurrence of multimeric circular DNA in senescent cultures. pp. 268-77. In: Engberg. J., et al., eds. *Specific Eukaryotic Genes*. Copenhagen, Munksgaard. , 1979. W3. AL36. 13th. 1978.

21. Dencher N.A., Goto S., Reifschneider N.H., Sugawa M., Krause F. (2006) Unraveling age-dependent variation of the mitochondrial proteome. *Ann N Y Acad Sci* 1067, 116-119
22. Deniaud A., Hoebeke J., Briand J.P., Muller S., Jacotot E., Brenner C. (2006) Peptido-targeting of the mitochondrial transition pore complex for therapeutic apoptosis induction. *Curr Pharm Des* 12, 4501-4511
23. Deocaris C.C., Kaul S.C., Wadhwa R. (2006) On the brotherhood of the mitochondrial chaperones mortalin and heat shock protein 60. *Cell Stress Chaperones* 11, 116-128
24. Ding Q., Dimayuga E., Keller J.N. (2006a) Proteasome regulation of oxidative stress in ageing and age-related diseases of the CNS. *Antioxid Redox Signal* 8, 163-172
25. Ding Q., Vaynman S., Souda P., Whitelegge J.P., Gomez-Pinilla F. (2006b) Exercise affects energy metabolism and neural plasticity-related proteins in the hippocampus as revealed by proteomic analysis. *Eur J Neurosci* 24, 1265-1276
26. Dolman N.J., Gerasimenko J.V., Gerasimenko O.V., Voronina S.G., Petersen O.H., Tepikin A.V. (2005) Stable Golgi-mitochondria complexes and formation of Golgi Ca(2+) gradients in pancreatic acinar cells. *J Biol Chem* 280, 15794-15799
27. Donati A., Taddei M., Cavallini G., Bergamini E. (2006) Stimulation of macroautophagy can rescue older cells from 8-OHdG mtDNA accumulation: a safe and easy way to meet goals in the SENS agenda. *Rejuvenation Res* 9, 408-412

28. Dufour, E., Boulay, J., Rincheval, V., and Sainsard-Chanet, A. (2000) A causal link between respiration and senescence in *Podospora anserina*. Proc. Natl. Acad. Sci U. S. A 97, 4138-4143.
29. Eriksen J.L., Wszolek Z., Petrucelli L. (2005) Molecular pathogenesis of Parkinson disease. Arch Neurol 62, 353-357
30. Esser, K., Kück, U., Stahl, U., and Tudzynski, P. (1981). Mitochondrial DNA and Senescence in *Podospora anserina*. Curr. Genet. 4, 83
31. Forner F., Foster L.J., Campanaro S., Valle G., Mann M. (2006) Quantitative proteomic comparison of rat mitochondria from muscle, heart, and liver. Mol Cell Proteomics 5, 608-619
32. Gillardon F (2006) Differential mitochondrial protein expression profiling in neurodegenerative diseases. Electrophoresis 27, 2814-2818
33. Gredilla R., Grief J., Osiewacz H.D. (2006) Mitochondrial free radical generation and lifespan control in the fungal ageing model *Podospora anserina*. Exp Gerontol 41, 439-447
34. Harman, D. (1956). Ageing: a theory based on free radical and radiation chemistry. J Gerontol 11, 298-300.
35. Hunzinger C., Wozny W., Schwall G.P., Poznanovic S., Stegmann W., Zengerling H., Schoepf R., Groebe K., Cahill M.A., Osiewacz H.D., Jagemann N., Bloch M., Dencher N.A., Krause F., Schratzenholz A. (2006) Comparative profiling of the mammalian mitochondrial proteome: multiple aconitase-2 isoforms including N-formylkynurenine modifications as part of a protein biomarker signature for reactive oxidative species. J Proteome Res 5, 625-633

36. Jacobs, H. T. (2003). The mitochondrial theory of ageing: dead or alive? Ageing Cell 2, 11-17
37. Jaffe E.A., Nachman R.L., Becker C.G., Minick C.R. (1973) Culture of human endothelial cells derived from umbilical veins: Identification by morphologic and immunologic criteria. J Clin Invest 52, 2745-2756
38. Jin J., Meredith G.E., Chen L., Zhou Y., Xu J., Shie F.S., Lockhart P., Zhang J. (2005) Quantitative proteomic analysis of mitochondrial proteins: relevance to Lewy body formation and Parkinson's disease. Brain Res Mol Brain Res 134, 119-138
39. Johnson D.T., Harris R.A., Blair P.V., Balaban R.S. (2006) Functional Consequences of Mitochondrial Proteome Heterogeneity. Am J Physiol Cell Physiol 292, C698-707
40. Kang D., Hamasaki N. (2003) Mitochondrial oxidative stress and mitochondrial DNA. Clin Chem Lab Med 41, 1281-1288
41. Kim K.B., Lee J.W., Lee C.S., Kim B.W., Choo H.J., Jung S.Y., Chi S.G., Yoon Y.S., Yoon G., Ko Y.G. (2006) Oxidation-reduction respiratory chains and ATP synthase complex are localized in detergent-resistant lipid rafts. Proteomics 6, 2444-2453
42. Koll, F., Begel, O., Keller, A.M., Vierny, C., and Belcour, L. (1984). Ethidium bromide rejuvenation of senescent cultures of *Podospora anserina*: Loss of senescence-specific DNA and recovery of normal mitochondrial DNA. Curr. Genet. 8, 127-134

43. Kowald, A. (2001). The mitochondrial theory of ageing. *Biol Signals Recept* 10, 162-175.
44. Kowald, A., Jendrach, M., Pohl, S., Bereiter-Hahn, J. and Hammerstein, P. (2005). On the relevance of mitochondrial fusions for the accumulation of mitochondrial deletion mutants: a modelling study. *Ageing Cell* 4, 273-283
45. Krause F., Reifschneider N.H., Goto S., Dencher N.A. (2005) Active oligomeric ATP synthases in mammalian mitochondria. *Biochem Biophys Res Commun* 329, 583-590
46. Krause F., Scheckhuber C.Q., Werner A., Rexroth S., Reifschneider N.H., Dencher N.A., Osiewacz H.D. (2004) Supramolecular organization of cytochrome c oxidase- and alternative oxidase-dependent respiratory chains in the filamentous fungus *Podospira anserina*. *J Biol Chem* 279, 26453-26461
47. Kraytsberg Y., Kudryavtseva E., McKee A.C., Geula C., Kowall N.W., Khrapko K. (2006) Mitochondrial DNA deletions are abundant and cause functional impairment in aged human substantia nigra neurons. *Nat Genet* 38, 518-520
48. Kück, U., Stahl, U., and Esser, K. (1981). Plasmid-like DNA is part of mitochondrial DNA in *Podospira anserina*. *Curr. Genet.* 3, 151-156
49. Kujoth, G. C., Hiona, A., Pugh, T. D., Someya, S., Panzer, K., Wohlgemuth, S. E., Hofer, T., Seo, A. Y., Sullivan, R., Jobling, W. A., *et al.* (2005). Mitochondrial DNA mutations, oxidative stress, and apoptosis in mammalian ageing. *Science* 309, 481-484
50. Laun, P., Pichova, A., Madeo, F., Fuchs, J., Ellinger, A., Kohlwein, S., Dawes, I., Frohlich, K. U., and Breitenbach, M. (2001). Aged mother cells of

Saccharomyces cerevisiae show markers of oxidative stress and apoptosis. *Mol*

Microbiol 39, 1166-1173

51. Lesnefsky E.J., Hoppel C.L. (2006) Oxidative phosphorylation and ageing. *Ageing Res Rev* 5, 402-433
52. Marin-Garcia J., Pi Y., Goldenthal M.J. (2006) Mitochondrial-nuclear Cross-talk in the Ageing and Failing Heart. *Cardiovasc Drugs Ther.* 20, 477-91
53. Marley K., Mooney D.T., Clark-Scannell G., Tong T.T., Watson J., Hagen T.M., Stevens J.F., Maier C.S. (2005) Mass tagging approach for mitochondrial thiol proteins. *J Proteome Res* 4, 1403-1412
54. McMahon K.A., Zhu M., Kwon S.W., Liu P., Zhao Y., Anderson R.G. (2006) Detergent-free caveolae proteome suggests an interaction with ER and mitochondria. *Proteomics* 6, 143-152
55. Miquel, J. (1991). An integrated theory of ageing as the result of mitochondrial-DNA mutation in differentiated cells. *Arch Gerontol Geriatr* 12, 99-117
56. Miquel, J., Binnard, R., and Fleming, J. E. (1983). Role of metabolic rate and DNA-repair in *Drosophila* ageing: implications for the mitochondrial mutation theory of ageing. *Exp Gerontol* 18, 167-171
57. Neubauer H., Clare S.E., Kurek R., Fehm T., Wallwiener D., Sotlar K., Nordheim A., Wozny W., Schwall G.P., Poznanovic S., Sastri C., Hunzinger C., Stegmann W., Schratzenholz A., Cahill M.A. (2006) Breast cancer proteomics by laser capture microdissection, sample pooling, 54-cm IPG IEF, and differential iodine radioisotope detection. *Electrophoresis* 27, 1840-1852

58. Osiewacz H.D. (2002) Ageing in fungi: role of mitochondria in *Podospora anserina*. *Mech Ageing Dev* 123, 755-764
59. Osiewacz H.D., Scheckhuber C.Q. (2006) Impact of ROS on ageing of two fungal model systems: *Saccharomyces cerevisiae* and *Podospora anserina*. *Free Radic Res* 40, 1350-1358
60. Osiewacz, H.D. (2002). Mitochondrial functions and ageing. *Gene* 286, 65-71
61. Osiewacz, H.D. and Esser, K. (1984). The mitochondrial plasmid of *Podospora anserina*: A mobile intron of a mitochondrial gene. *Curr. Genet.* 8, 299-305
62. Osiewacz, H.D. and Hermanns, J. (1992). The role of mitochondrial DNA rearrangements in ageing and human diseases [see comments]. *Ageing (Milano)* 4, 273-286
63. Piec I., Listrat A., Alliot J., Chambon C., Taylor R.G., Bechet D. (2005) Differential proteome analysis of ageing in rat skeletal muscle. *FASEB J* 19, 1143-1145
64. Poon H.F., Calabrese V., Calvani M., Butterfield D.A. (2006a) Proteomics analyses of specific protein oxidation and protein expression in aged rat brain and its modulation by L-acetylcarnitine: insights into the mechanisms of action of this proposed therapeutic agent for CNS disorders associated with oxidative stress. *Antioxid Redox Signal* 8, 381-394
65. Poon H.F., Shepherd H.M., Reed T.T., Calabrese V., Stella A.M., Pennisi G., Cai J., Pierce W.M., Klein J.B., Butterfield D.A. (2006b) Proteomics analysis provides insight into caloric restriction mediated oxidation and expression of brain proteins associated with age-related impaired cellular processes:

Mitochondrial dysfunction, glutamate dysregulation and impaired protein synthesis. *Neurobiol Ageing* 27, 1020-1034

66. Poon H.F., Vaishnav R.A., Butterfield D.A., Getchell M.L., Getchell T.V. (2005) Proteomic identification of differentially expressed proteins in the ageing murine olfactory system and transcriptional analysis of the associated genes. *J Neurochem* 94, 380-392
67. Poon H.F., Vaishnav R.A., Getchell T.V., Getchell M.L., Butterfield D.A. (2006c) Quantitative proteomics analysis of differential protein expression and oxidative modification of specific proteins in the brains of old mice. *Neurobiol Ageing* 27, 1010-1019
68. Poznanovic S., Wozny W., Schwall G.P., Sastri C., Hunzinger C., Stegmann W., Schrattenholz A., Buchner A., Gangnus R., Burgemeister R., Cahill M.A. (2005) Differential radioactive proteomic analysis of microdissected renal cell carcinoma tissue by 54 cm isoelectric focusing in serial immobilized pH gradient gels. *J Proteome Res* 4, 2117-2125
69. Prokisch H., Andreoli C., Ahting U., Heiss K., Ruepp A., Scharfe C., Meitinger T. (2006) MitoP2: the mitochondrial proteome database--now including mouse data. *Nucleic Acids Res* 34, D705-D711
70. Reifschneider N.H., Goto S., Nakamoto H., Takahashi R., Sugawa M., Dencher N.A., Krause F. (2006) Defining the mitochondrial proteomes from five rat organs in a physiologically significant context using 2D blue-native/SDS-PAGE. *J Proteome Res* 5, 1117-1132

71. Reinders J., Zahedi R.P., Pfanner N., Meisinger C., Sickmann A. (2006) Toward the complete yeast mitochondrial proteome: multidimensional separation techniques for mitochondrial proteomics. *J Proteome Res* 5, 1543-1554
72. Rickwood D., Hayes A. (1984) An evaluation of methods used to prepare yeast mitochondria for transcriptional studies. *Prep Biochem* 14, 163-171
73. Rottenberg H. (2006) Longevity and the evolution of the mitochondrial DNA-coded proteins in mammals. *Mech Ageing Dev* 127, 748-760
74. Ruiz-Romero C., Lopez-Armada M.J., Blanco F.J. (2006) Mitochondrial proteomic characterization of human normal articular chondrocytes. *Osteoarthritis Cartilage* 14, 507-518
75. Sanz A., Pamplona R., Barja G. (2006) Is the mitochondrial free radical theory of ageing intact? *Antioxid Redox Signal* 8, 582-599
76. Scheckhuber C.Q., Erjavec N., Tinazli A., Hamann A, Nystrom T., Osiewacz H.D. (2007) Reducing mitochondrial fission results in increased life span and fitness of two fungal ageing models. *Nat Cell Biol* 9, 99-105
77. Schieke S.M., Phillips D., McCoy J.P., Jr., Aponte A.M., Shen R.F., Balaban R.S., Finkel T. (2006) The mammalian target of rapamycin (mTOR) pathway regulates mitochondrial oxygen consumption and oxidative capacity. *J Biol Chem* 281, 27643-27652
78. Schratzenholz A., Groebe K. (2007) What does it need to be a biomarker? Relationships between resolution, differential quantification and statistical validation of protein surrogate biomarkers. *Electrophoresis*, May 22, Epub ahead of print

79. Schrattenholz A., Soskic V. (2006) NMDA receptors are not alone: dynamic regulation of NMDA receptor structure and function by neuregulins and transient cholesterol-rich membrane domains leads to disease-specific nuances of glutamate-signalling. *Curr Top Med Chem* 6, 663-686
80. Schulte, E., Kück, U., and Esser, K. (1988). Extrachromosomal mutants from *Podospira anserina*: Permanent vegetative growth in spite of multiple recombination events in the mitochondrial genome. *Mol. Gen. Genet.* 211, 342-349
81. Simat T.J., Steinhart H. (1998) Oxidation of Free Tryptophan and Tryptophan Residues in Peptides and Proteins. *J Agric Food Chem* 46, 490-498
82. Singh K.K. (2006) Mitochondrial damage checkpoint, ageing, and cancer. *Ann N Y Acad Sci* 1067, 182-190
83. Soskic V., Klemm M., Proikas-Cezanne T., Schwall GP., Poznanovic S., Stegmann W., Groebe K., Zengerling H., Schoepf R., Burnet M., Schrattenholz A. (2007) A connection between the mitochondrial permeability transition pore, autophagy and cerebral amyloidogenesis. submitted
84. Soti C., Csermely P. (2007) Ageing cellular networks: Chaperones as major participants. *Exp Gerontol.* 42, 113-139
84. Stahl, U., Lemke, P.A., Tudzynski, P., Kück, U. and Esser, K. (1978) Evidence for plasmid like DNA in a filamentous fungus, the ascomycete *Podospira anserina*. *Mol. Gen. Genet.* 162, 341-343

85. Stockl, P., Hutter, E., Zwerschke, W., and Jansen-Durr, P. (2006). Sustained inhibition of oxidative phosphorylation impairs cell proliferation and induces premature senescence in human fibroblasts. *Exp Gerontol* 41, 674-682
86. Stumpferl, S.W., Stephan, O. and Osiewacz, H.D. (2004). Impact of a disruption of a pathway delivering copper to mitochondria on *Podospora anserina* metabolism and life span. *Eukaryotic Cell* 3, 200-211
87. Sultana R., Boyd-Kimball D., Poon H.F., Cai J., Pierce W.M., Klein J.B., Merchant M., Markesbery W.R., Butterfield D.A. (2006) Redox proteomics identification of oxidized proteins in Alzheimer's disease hippocampus and cerebellum: an approach to understand pathological and biochemical alterations in AD. *Neurobiol Ageing* 27, 1564-1576
88. Takahashi R. and Goto S. (1987) Influence of dietary restriction on accumulation of heat-labile enzyme molecules in the liver and brain of mice, *Arch. Biochem. Biophys.* 257 200–206
89. Terman A., Brunk U.T. (2006) Oxidative stress, accumulation of biological 'garbage', and ageing. *Antioxid Redox Signal* 8, 197-204
90. Trifunovic, A., Hansson, A., Wredenberg, A., Rovio, A. T., Dufour, E., Khvorostov, I., Spelbrink, J. N., Wibom, R., Jacobs, H. T., and Larsson, N. G. (2005). Somatic mtDNA mutations cause ageing phenotypes without affecting reactive oxygen species production. *Proc Natl Acad Sci U S A* 102, 17993-17998
91. Trifunovic, A., Wredenberg, A., Falkenberg, M., Spelbrink, J. N., Rovio, A. T., Bruder, C. E., Bohlooly, Y. M., Gidlof, S., Oldfors, A., Wibom, R., *et al.* (2004).

Premature ageing in mice expressing defective mitochondrial DNA polymerase.

Nature 429, 417-423

92. Unterluggauer H., Hampel B., Zwerschke W., Jansen-Durr P. (2003)
Senescence-associated cell death of human endothelial cells: the role of
oxidative stress. *Exp Gerontol* 38, 1149-1160
93. Vijg, J. (2000). Somatic mutations and ageing: a re-evaluation. *Mutat Res* 447,
117-135
94. Vo T.D., Palsson B. (2007) Building the power house: Recent advances in
mitochondrial studies through proteomics and systems biology. *Am J Physiol
Cell Physiol* 292, C164-177
95. Vogt J.A., Hunzinger C., Schroer K., Holzer K., Bauer A., Schratzenholz A.,
Cahill M.A., Schillo S., Schwall G., Stegmann W., Albuszies G. (2005)
Determination of fractional synthesis rates of mouse hepatic proteins via
metabolic ¹³C-labeling, MALDI-TOF MS and analysis of relative isotopologue
abundances using average masses. *Anal Chem* 77, 2034-2042
96. Wallace, D. C. (2001). A mitochondrial paradigm for degenerative diseases and
ageing. *Novartis Found Symp* 235, 247-263; discussion 263-246
97. Wang, W., Yang, X., Lopez De Silanes, I., Carling, D., and Gorospe, M. (2003).
Increased AMP: ATP ratio and AMP-activated kinase activity during cellular
senescence linked to reduced HuR function. *J Biol Chem* 278, 27016-27023
98. Weinreb O., Drigues N., Sagi Y., Reznick A.Z., Amit T., Youdim M.B. (2007) The
Application of Proteomics and Genomics to the Study of Age-Related
Neurodegeneration and Neuroprotection. *Antioxid Redox Signal* 9, 169-179

99. Wozny W., Schroer K., Schwall G., Poznanovic S., Stegmann W., Dietz K., Rogatsch H., Schaefer G., Huebl H., Klocker H., Schratzenholz A., Cahill M.A. (2007) Differential Radioactive Quantification of Protein Abundance Ratios Between Benign and Malignant Prostate Tissues: Cancer Association of Annexin A3. *Proteomics* 7, 313-322
100. Yonally S.K., Capaldi R.A. (2006) The F(1)F(0) ATP synthase and mitochondrial respiratory chain complexes are present on the plasma membrane of an osteosarcoma cell line: An immunocytochemical study. *Mitochondrion* 6, 305-314
101. Zwerschke, W., Mazurek, S., Stockl, P., Hutter, E., Eigenbrodt, E., and Jansen-Durr, P. (2003). Metabolic analysis of senescent human fibroblasts reveals a role for adenosine monophosphate in cellular senescence. *Biochem J* 376, 403-411

Table 1: Redundant posttranslational age-related isoforms from the different models
in three species:

Species	Description	Theoretical		Experiment		Spot ID
		MW	pI	MW	pI	
Podospora anserina	ATP synthase β chain, mitochondrial precursor	60792	5.5	58000 14800	4.6-4.7 4.87	904, 907, 917, 920, 2249
	ATP synthase subunit 4, mitochondrial precursor	26458 55802	9.2	25000	5.6	1192
	ATP synthase oligomycin sensitivity conferral protein- like protein	23573	9.6	24000	8.5	1555
	ATP synthase γ chain, mitochondrial precursor	33019	8.9	32000	6.8	1337
Rattus norvegicus	ATP synthase, mitochondrial F1 complex, β subunit	56318	5.0	53000, 33000 59000, 43000	4.9, 4.8 5.1, 5.1	1436, 1470, 1685, 1694, 1715, 2476,
Homo sapiens	ATPase 5A1 protein	49119	9.2	57500, 56500	6.8, 7.0	760, 762, 1225, 1255
	ATP synthase, H ⁺ transporting, mitochondrial F1 complex, α subunit, precursor	61456	9.2	56.500, 55000	6.85, 6.6	
Podospora anserina	Putative SAM-dependent O- methyltransferase (PaMTH1)	27774	5.4	27000	5.2, 5.35	1079, 1092
Homo sapiens	Reticulocalbin 1, precursor	38866		47500	4.6-4.8	xxx
	Reticulocalbin 3	37470				
	Reticulocalbin precursor	37401				

Table S1

Juvenile versus senescent *Podospora anserina* (mitochondrial preparation)
All accession numbers are from *Podospora anserina* if not stated otherwise

Protein	Identification						Quantification			
	Accession Number	PMF score	Mass	pI	exp. mass	exp. pI	Juv (%)	Sen (%)	StdDev (%)	p-value
SC_J_chrm5.seq:55882..56625	ps 27328	71	22181	9.6	16500	5.2	72.0	28.0	14.433	<0.0001
3-hydroxyacyl-CoA dehydrogenase, NAD binding domain (SC_A_chrm2.seq:1878728..1879998)	ps 22964	151	35136	9.2	31000	7.8	71.1	28.9	5.5467	<0.0001
Isocitrate dehydrogenase subunit 1, mitochondrial precursor (SC_B_chrm1.seq:1727818..1729170)	ps 20585	211	43057	9	44333	7.067	71.1	28.9	8.04	<0.0001
Acetyl-CoA acetyltransferase (SC_A_chrm6.seq:563339..564758)	ps 27514	147	45657	8.9	44333	7.067				
Ubiquinol-cytochrome-c reductase complex core protein 2, mitochondrial precursor. (SC_B_chrm6.seq:411876..413451)	ps 27828	110	46451	7.8	44333	7.067				
Acetyl-CoA acetyltransferase (SC_A_chrm6.seq:563339..564758)	ps 27514	197	45657	8.9	44333	7.167	70.4	29.6	6.0058	<0.0001
Isocitrate dehydrogenase subunit 1, mitochondrial precursor (SC_B_chrm1.seq:1727818..1729170)	ps 20585	135	43057	9	44333	7.167				
ATP synthase beta chain, mitochondrial precursor (SC_B_chrm6.seq:781183..783469)	ps 27916	122	60792	5.5	58333	4.6	67.8	32.2	7.945	<0.0001
Malate dehydrogenase, mitochondrial precursor (SC_B_chrm3.seq:251337..251966)	ps 24151	124	22580	5.8	35000	7.5	67.2	32.8	7.2148	<0.0001
Hypothetical protein [Neurospora crassa OR74A]	gi 32407475	110	36027	9.1	35000	7.5				
Hypothetical protein MG09367.4 [Magnaporthe grisea 70-15]	gi 39960255	110	35878	8.3	35000	7.5				
NADH-quinone oxidoreductase (SC_B_chrm1.seq:1943172..	ps 20639	126	21865	5.4	24333	5.4	66.8	33.2	8.8648	<0.0001

.1943841)										
Methylmalonate-semialdehyde dehydrogenase, mitochondrial precursor (SC_B_chrm1.seq:2405475..2407298)	ps 20766	151	63908	8.3	63333	5.9	66.7	33.3	8.2418	<0.0001
Acyl-CoA dehydrogenase (SC_D_chrm6.seq:109461..111164)	ps 28197	152	61265	8.2	50500	5.2	66.6	33.4	7.4067	<0.0001
Flavohemoglobin (SC_A_chrm5.seq:647906..649171)	ps 26217	113	46652	5.3	50500	5.2				
Hypothetical protein [Neurospora crassa OR74A]	gi 85106801	108	47942	7.9	50500	5.2				
Hypothetical protein MG09367.4 [Magnaporthe grisea 70-15]	gi 39960255	131	35878	8.3	35000	7.55	66.3	33.7	10.942	0.0020
Malate dehydrogenase, mitochondrial precursor [Chaetomium globosum CBS 148.51]	gi 88181085	120	35865	8.6	35000	7.55				
Malate dehydrogenase, mitochondrial precursor [Chaetomium globosum CBS 148.51]. (SC_B_chrm3.seq:251337..251966)	ps 24151	115	22580	5.8	35000	7.55				
ATP synthase beta chain, mitochondrial precursor (SC_B_chrm6.seq:781183..783469)	ps 27916	249	60792	5.5	58000	4.633	66.2	33.8	6.0773	<0.0001
Electron transfer flavoprotein subunit alpha (SC_A_chrm6.seq:473832..474884)	ps 27491	213	36424	5.8	34000	5.1	65.8	34.2	7.0367	<0.0001
Glycine cleavage system H protein (SC_A_chrm2.seq:2279444..2280030)	ps 23086	98	18719	4.8	18000	4.4	65.7	34.3	7.1411	<0.0001
Glycine cleavage system H protein (SC_A_chrm2.seq:2279444..2280030)	ps 23086	84	18719	4.8	17500	4.4	65.2	34.8	7.15	<0.0001
Peptidylprolyl isomerase (SC_A_chrm2.seq:1458028..1458541)	ps 22843	121	15688	9.3	16666	5.367	64.9	35.1	6.2908	<0.0001
ATP synthase beta chain, mitochondrial precursor (SC_B_chrm6.seq:781183..783469)	ps 27916	282	60792	5.5	57666	4.7	64.2	35.8	6.8307	<0.0001
Putative peroxiredoxin (SC_F_chrm5.seq:280296..280916)	ps 26871	125	20204	7.8	16666	5.367	63.9	36.1	5.4021	<0.0001
Manganese superoxide dismutase (SC_A_chrm5.seq:663911..664819)	ps 26221	155	25479	6.5	22666	5.5	63.6	36.4	7.1141	<0.0001

Enoyl-CoA hydratase, putative (SC_C_chrm7.seq:1806496..1807056)	ps 29563	152	20387	6.2	28666	6.567	63.2	36.8	6.3754	0.0003
Glycine cleavage system H protein (SC_A_chrm2.seq:2279444..2280030)	ps 23086	81	18719	4.8	18000	4.25	63.2	36.8	8.1601	<0.0001
ATP synthase subunit 4, mitochondrial precursor (SC_E_chrm1.seq:1244142..1245072)	ps 21763	162	26458	9.2	24000	5.6	63.0	37.0	7.9239	<0.0001
Cytochrome c oxidase polypeptide IV, mitochondrial precursor (SC_A_chrm7.seq:191738..192859)	ps 28599	107	20630	6.2	19666	4.967	62.8	37.2	7.1631	<0.0001
Ubiquinol-cytochrome-c reductase complex core protein 2, mitochondrial precursor. (SC_B_chrm6.seq:411876..413451)	ps 27828	202	46451	7.8	44666	6.967	61.5	38.5	9.166	0.0054
Isocitrate dehydrogenase subunit 1, mitochondrial precursor (SC_B_chrm1.seq:1727818..1729170)	ps 20585	170	43057	9	44666	6.967				
Acetyl-CoA acetyltransferase (SC_A_chrm6.seq:563339..564758)	ps 27514	96	45657	8.9	44666	6.967				
Mitochondrial import receptor subunit TOM20 (MOM19 protein) (SC_A_chrm6.seq:652966..653662)	ps 27547	81	20350	4.8	18000	4.8	61.4	38.6	6.209	<0.0001
Cytochrome c subunit Vb (SC_A_chrm7.seq:191738..192859)	ps 28599	111	20630	6.2	18333	4.967	59.8	40.2	6.8626	<0.0001
ATP synthase beta chain, mitochondrial precursor (SC_B_chrm6.seq:781183..783469)	ps 27916	310	60792	5.5	57333	4.7	59.4	40.6	9.493	0.0013
Heat shock protein SSC1, mitochondrial precursor (SC_A_chrm6.seq:904733..906927)	ps 27612	106	72862	5.9	33333	4.9	40.9	59.1	16.392	0.0427
Vacuolar-ATPase (SC_E_chrm1.seq:962729..963867)	ps 21700	85	37859	9.1	22000	6.6	37.7	62.3	6.6932	0.0006
Ubiquinol-cytochrome c reductase complex core protein I (SC_B_chrm1.seq:1974671..1976261)	ps 20652	251	48004	4.9	52666	5.067	37.2	62.8	10.405	0.0005
Heat shock protein SSC1, mitochondrial precursor (SC_A_chrm6.seq:904733..906927)	ps 27612	74	72862	5.9	52666	5.067				

Elongation factor 1-beta [Aspergillus terreus NIH2624]. (SC_C_chrm5.seq:162845.. 163892)	ps 26538	67	25342	4.3	37000	4.3	36.5	63.5	8.0793	<0.0001
ATP synthase oligomycin sensitivity conferral protein- like protein (SC_B_chrm3.seq:2193212. .2194235)	ps 24700	194	23573	9.6	22666	8.5	35.2	64.8	7.0871	0.0002
ATP synthase beta chain, mitochondrial precursor (SC_B_chrm6.seq:781183.. 783469)	ps 27916	75	60792	5.5	15000	4.8	35.1	64.9	6.8754	<0.0001
Vacuolar-ATPase (SC_E_chrm1.seq:962729.. 963867)	ps 21700	73	37859	9.1	22000	6.9	32.8	67.2	7.7993	0.0002
ATP synthase gamma chain, mitochondrial precursor (SC_C_chrm1.seq:218135.. 219388)	ps 20945	119	33019	8.9	31000	6.85	32.4	67.6	6.7909	<0.0001
SC_D_chrm4.seq:604601..6 05847	ps 25644	184	42440	9.4	39666	6.4	32.0	68.0	4.4705	<0.0001
Hypothetical protein CHGG_09308 [Chaetomium globosum CBS 148.51]	gi 88177826	117	33545	9	39666	6.4				
SC_A_chrm2.seq:4588577.. 4589920	ps 23766	67	42347	4.7	67500	4.6				
Aspartate aminotransferase, mitochondrial precursor (SC_C_chrm3.seq:293121.. 294666)	ps 25020	202	43289	8.3	41333	6.933	29.5	70.5	19.133	0.0123
Vacuolar protease A precursor (SC_F_chrm5.seq:579358.. 580684)	ps 26947	113	43599	5	46666	4.5	28.9	71.1	7.4027	<0.0001
SC_A_chrm2.seq:4588577.. 4589920	ps 23766	72	42347	4.7	70000	4.6	28.9	71.1	7.0036	<0.0001
Nucleoside diphosphate kinase (SC_A_chrm2.seq:3204186.. .3204993)	ps 23368	153	17062	7.8	15666	7.167	28.6	71.4	6.0651	<0.0001
Putative mitochondrial cyclophilin 1 (SC_B_chrm1.seq:1416610.. .1417548)	ps 20492	122	26116	8.6	18333	5.6	23.5	76.5	6.5778	<0.0001
Putative SAM-dependent O- methyltransferase	gi 9968599	140	27774	5.2	26666	5.333	18.4	81.6	8.41	<0.0001
Putative SAM-dependent O- methyltransferase. (SC_A_chrm2.seq:2823633.. .2824514)	ps 23254	90	28975	7	26666	5.333				
Putative SAM-dependent O- methyltransferase	gi 9968599	131	27774	5.2	26666	5.2	17.6	82.4	7.084	<0.0001
Putative SAM-dependent O- methyltransferase. (SC_A_chrm2.seq:2823633.. .2824514)	ps 23254	102	28975	7	26666	5.2				

Disulfide isomerase (SC_C_chrm1.seq:492241.. 493831)	ps 21020	271	56166	4.8	66333	4.7	11.1	88.9	7.3024	<0.0001
Disulfide isomerase (SC_C_chrm1.seq:492241.. 493831)	ps 21020	113	56166	4.8	68333	4.633	10.9	89.1	6.1069	<0.0001
SC_A_chrm2.seq:4588577.. 4589920	ps 23766	66	42347	4.7	68333	4.633				
Pyruvate dehydrogenase E1 subunit beta (SC_E_chrm1.seq:550743.. 552061)	ps 21580	87	41423	6.1	16000	5.4	8.2	91.8	2.512	<0.0001

Table S2

Rat brain 5 months versus 17 months (mitochondrial preparation)
All accession numbers are from Rattus norvegicus if not stated otherwise

Protein	Identification						Quantification			
	Accession Number	PMF score	Mass	pI	exp. mass	exp. pI	5Mo (%)	17Mo (%)	StdDev (%)	p-value
ATP synthase, H+ transporting, mitochondrial F1 complex, beta subunit	gi 54792127	275	56318	5	53000	4.9	63.2	36.8	6.3252	0.0006
Tubb5 protein	gi 38014544	117	24787	4.7	36000	4.95	37.2	62.8	2.5173	<0.0001
Tubb2 protein [Mus musculus]	gi 13097483	87	34688	4.5	36000	4.95				
Tubulin beta chain 15 - rat	gi 92930	77	51322	4.5	36000	4.95				
Calretinin [Mus musculus]	gi 393387	116	22406	4.6	29000	4.8	40.1	59.9	5.8426	0.0020
Calbindin 2	gi 16758892	100	31739	4.7	29000	4.8	57.3	42.7	6.6337	0.0168
Neurofilament, light polypeptide	gi 13929098	164	61475	4.3	61000	5.2				
Tubulin alpha	gi 223556	130	52335	4.7	61000	5.2	59.8	40.2	8.3588	0.0125
Gamma-actin [Mus musculus]	gi 809561	139	42055	5.6	50000	5.5				
Actin beta - rat	gi 71620	138	42786	5.2	50000	5.5	39.2	60.8	7.7569	0.0056
COP9 signalosome subunit 4 [Mus musculus]	gi 6753490	109	47141	5.6	48000	5.5				
Guanine nucleotide-binding protein alpha subunit	gi 204444	77	37040	5.3	38000	5.1	56.3	43.7	3.882	0.0026
GTP-binding protein alpha o	gi 8394152	75	41814	5.2	38000	5.1	59.7	40.3	5.1443	0.0011
Tubulin beta chain 15 - rat	gi 92930	99	51322	4.5	39500	5.3				
Crystallin, mu	gi 56789444	98	34064	5.2	39500	5.3				
Tubulin alpha	gi 223556	71	52335	4.7	39500	5.3	57.4	42.6	1.6752	<0.0001
Eno1 protein	gi 50926833	83	48161	6.5	56000	6.1				
Malate dehydrogenase, mitochondrial	gi 42476181	185	37077	8.9	36000	7.6				
Similar to hemoglobin alpha chain	gi 34870607	77	15806	8.5	15000	7.3	41.6	58.4	6.5707	0.0084

Table S3
Rat brain 5 months versus 31 months (mitochondrial preparation)
All accession numbers are from Rattus norvegicus if not stated otherwise

Protein	Identification						Quantification			
	Accession Number	PMF score	Mass	pI	exp. Mass	exp. pI	5Mo (%)	31Mo (%)	StdDev (%)	p-value
Ubiquilin 1	gi 48675852	84	61975	4.6	74000	4.7	63.1	36.9	6.5456	0.0110
Tubulin alpha	gi 223556	90	52335	4.7	63000	5	57.7	42.3	8.556	0.0378
Rab GDP dissociation inhibitor alpha (Rab GDI alpha) (GDI-1)	gi 1707888	73	52275	4.8	63000	5				
Tubulin beta chain 15 - rat	gi 92930	71	51322	4.5	63000	5				
Unknown (protein for MGC:94172)	gi 50926985	89	48314	4.5	61500	4.7	64.4	35.6	6.3856	0.0004
Type II cAMP-dependent protein kinase regulatory subunit	gi 206671	75	47202	4.6	61500	4.7				
ATP synthase, H+ transporting, mitochondrial F1 complex, beta subunit	gi 54792127	275	56318	5	53000	4.9	62.8	37.2	7.8943	0.0025
Tubb2 protein [Mus musculus]	gi 13097483	103	34688	4.5	38000	4.8	58.8	41.2	10.578	0.0499
Tubulin beta chain 15 - rat	gi 92930	92	51322	4.5	38000	4.8				
Tubb5 protein	gi 38014544	117	24787	4.7	36000	4.95	55.9	44.1	5.4041	0.0175
Tubb2 protein [Mus musculus]	gi 13097483	87	34688	4.5	36000	4.95				
tubulin beta chain 15 - rat	gi 92930	77	51322	4.5	36000	4.95				
Tyrosine 3/tryptophan 5 - monooxygenase activation protein, eta polypeptide	gi 6981710	82	28725	4.5	30000	4.8	64.9	35.1	3.7409	<0.0001
Hsc70-ps1	gi 56385	86	71593	5.2	80000	5	64.0	36.0	5.1318	0.0001
Heat shock protein 8 [Mus musculus]	gi 55250073	86	71536	5.2	80000	5				
Internexin, alpha	gi 9506811	381	56613	4.9	73000	5.2	67.1	32.9	15.393	0.0161
Tubulin alpha	gi 223556	140	52335	4.7	63000	5.1	60.4	39.6	6.248	0.0022
Tubulin alpha	gi 223556	162	52335	4.7	63000	5.1	57.9	42.1	6.7756	0.0132
Tubulin alpha	gi 223556	156	52335	4.7	63000	5.1	57.9	42.1	7.5551	0.0208
Tubulin alpha	gi 223556	159	52335	4.7	64000	5.1	59.2	40.8	7.151	0.0082
Tubulin beta chain 15 - rat	gi 92930	106	51322	4.5	64000	5.1				
Tubulin alpha	gi 223556	142	52335	4.7	64000	5.1	59.1	40.9	5.5095	0.0023
Tubulin beta chain 15 - rat	gi 92930	84	51322	4.5	64000	5.1				
Neurofilament, light polypeptide	gi 13929098	164	61475	4.3	61000	5.2	63.3	36.7	6.9854	0.0010
Tubulin alpha	gi 223556	130	52335	4.7	61000	5.2				
Tubulin alpha	gi 223556	155	52335	4.7	60000	5.1	61.3	38.7	4.5432	0.0002
Enolase 2, gamma	gi 37805239	143	48350	4.8	51000	5	59.9	40.1	9.9273	0.0257
Gamma-actin [Mus musculus]	gi 809561	139	42055	5.6	50000	5.5	61.0	39.0	7.4007	0.0039
Actin beta - rat	gi 71620	138	42786	5.2	50000	5.5				
Gamma-actin [Mus musculus]	gi 809561	157	42055	5.6	49500	5.4	68.3	31.7	5.564	<0.0001
Actin beta - rat	gi 71620	155	42786	5.2	49500	5.4				
Gamma-actin [Mus musculus]	gi 809561	187	42055	5.6	51000	5.2	60.4	39.6	11.566	0.0382

Actin beta - rat	gi 71620	186	42786	5.2	51000	5.2					
COP9 signalosome subunit 4 [Mus musculus]	gi 6753490	109	47141	5.6	48000	5.5	30.0	70.0	7.2891	0.0001	
Gamma-actin [Mus musculus]	gi 809561	80	42055	5.6	48000	5.3	65.4	34.6	5.5958	0.0001	
Actin beta - rat	gi 71620	79	42786	5.2	48000	5.3					
Isocitrate dehydrogenase 3 (NAD+) alpha	gi 16758446	171	41005	6.9	45000	5.5	57.9	42.1	8.619	0.0352	
ATP synthase, H+ transporting, mitochondrial F1 complex, beta subunit	gi 54792127	80	56318	5	43000	5.1	58.2	41.8	7.2202	0.0145	
Guanine nucleotide-binding protein alpha subunit	gi 204444	77	37040	5.3	38000	5.1	65.7	34.3	5.1981	<0.0001	
GTP-binding protein alpha o	gi 8394152	75	41814	5.2	38000	5.1					
Acidic ribosomal protein P0	gi 450370	73	34725	6.2	40000	5.6	60.0	40.0	6.9207	0.0046	
Similar to Beta-soluble NSF attachment protein (SNAP-beta) (N-ethylmaleimide-sensitive factor attachment protein, beta)	gi 34859344	120	40357	6.1	37000	5.3	59.5	40.5	9.7324	0.0286	
Similar to heme-binding protein	gi 34858543	97	21465	5.1	25000	5.2	57.1	42.9	7.26	0.0279	
Ubiquitin-conjugating enzyme E2N (homologous to yeast UBC13)	gi 58477429	105	17290	6.5	16000	5.7	61.9	38.1	6.8741	0.0017	
Cytochrome c oxidase subunit Va preprotein	gi 55971	89	16828	6.5	15000	5.2	59.9	40.1	7.2557	0.0061	
Cytochrome c oxidase, subunit Va [Mus musculus]	gi 21707954	89	16800	6.5	15000	5.2					
Eno1 protein	gi 50926833	83	48161	6.5	56000	6.1	57.8	42.2	6.3626	0.0103	
Malate dehydrogenase, mitochondrial	gi 42476181	185	37077	8.9	36000	7.6	55.8	44.2	5.6511	0.0236	

Table S4
Rat brain 17 months versus 31 months(mitochondrial preparation)
All accession numbers are from Rattus norvegicus if not stated otherwise

Protein	Identification						Quantification			
	Accession Number	PMF score	Mass	pI	exp. Mass	exp. pI	17Mo (%)	31Mo (%)	StdDev (%)	p-value
Tubulin alpha	gi 223556	90	52335	4.7	63000	5	58.9	41.1	9.0029	0.0272
Rab GDP dissociation inhibitor alpha (Rab GDI alpha) (GDI-1)	gi 1707888	73	52275	4.8	63000	5				
Tubulin beta chain 15 - rat	gi 92930	71	51322	4.5	63000	5	63.6	36.4	5.551	0.0002
Unknown (protein for MGC:94172)	gi 50926985	89	48314	4.5	61500	4.7				
Type II cAMP-dependent protein kinase regulatory subunit	gi 206671	75	47202	4.6	61500	4.7	58.1	41.9	5.872	0.0060
Tubb2 protein [Mus musculus]	gi 13097483	103	34688	4.5	38000	4.8				
Tubulin beta chain 15 - rat	gi 92930	92	51322	4.5	38000	4.8	68.1	31.9	4.5623	<0.0001
Tubb5 protein	gi 38014544	117	24787	4.7	36000	4.95				
Tubb2 protein [Mus musculus]	gi 13097483	87	34688	4.5	36000	4.95				
Tubulin beta chain 15 - rat	gi 92930	77	51322	4.5	36000	4.95	62.3	37.7	4.6227	0.0001
Tyrosine 3/tryptophan 5 - monooxygenase activation protein, eta polypeptide	gi 6981710	82	28725	4.5	30000	4.8				
Calretinin [Mus musculus]	gi 393387	116	22406	4.6	29000	4.8	61.0	39.0	5.6596	0.0009
Calbindin 2	gi 16758892	100	31739	4.7	29000	4.8				
Vacuolar adenosine triphosphatase subunit B	gi 1184661	106	57788	5.5	69000	5.6	54.9	45.1	5.612	0.0418
Glucose regulated protein, 58 kDa	gi 38382858	87	58004	6.1	69000	5.6				
Tubulin alpha	gi 223556	140	52335	4.7	63000	5.1	58.4	41.6	3.9629	0.0005
Tubulin alpha	gi 223556	162	52335	4.7	63000	5.1	55.7	44.3	5.1568	0.0170
Tubulin alpha	gi 223556	156	52335	4.7	63000	5.1	56.5	43.5	6.9693	0.0341
Tubulin alpha	gi 223556	159	52335	4.7	64000	5.1	59.1	40.9	5.2161	0.0017
Tubulin beta chain 15 - rat	gi 92930	106	51322	4.5	64000	5.1	55.8	44.2	6.6918	0.0444
Tubulin alpha	gi 223556	142	52335	4.7	64000	5.1				
Tubulin beta chain 15 - rat	gi 92930	84	51322	4.5	64000	5.1	56.4	43.6	3.2626	0.0009
Neurofilament, light polypeptide	gi 13929098	164	61475	4.3	61000	5.2				
Tubulin alpha	gi 223556	130	52335	4.7	61000	5.2	57.6	42.4	5.1025	0.0040
Tubulin alpha	gi 223556	155	52335	4.7	60000	5.1				
Gamma-actin [Mus musculus]	gi 809561	157	42055	5.6	49500	5.4	67.4	32.6	6.1202	<0.0001
Actin beta - rat	gi 71620	155	42786	5.2	49500	5.4				
Gamma-actin [Mus musculus]	gi 809561	187	42055	5.6	51000	5.2	59.8	40.2	8.5599	0.0143
Actin beta - rat	gi 71620	186	42786	5.2	51000	5.2				
COP9 signalosome subunit 4 [Mus musculus]	gi 6753490	109	47141	5.6	48000	5.5	39.8	60.2	4.1461	0.0002
Gamma-actin [Mus musculus]	gi 809561	80	42055	5.6	48000	5.3	62.4	37.6	6.2746	0.0008
Actin beta - rat	gi 71620	79	42786	5.2	48000	5.3				

Isocitrate dehydrogenase 3 (NAD+) alpha	gi 16758446	171	41005	6.9	45000	5.5	57.6	42.4	8.1177	0.0339
ATP synthase, H+ transporting, mitochondrial F1 complex, beta subunit	gi 54792127	80	56318	5	43000	5.1	60.0	40.0	8.1932	0.0105
GTP-binding protein alpha o	gi 8394152	99	41814	5.2	42000	5	57.6	42.4	6.0174	0.0093
ATP synthase, H+ transporting, mitochondrial F1 complex, beta subunit	gi 54792127	73	56318	5	42000	5				
Guanine nucleotide-binding protein alpha subunit	gi 204444	77	37040	5.3	38000	5.1	59.9	40.1	5.7678	0.0019
GTP-binding protein alpha o	gi 8394152	75	41814	5.2	38000	5.1				
Acidic ribosomal protein P0	gi 450370	73	34725	6.2	40000	5.6	56.3	43.7	7.246	0.0447
Tubulin beta chain 15 - rat	gi 92930	99	51322	4.5	39500	5.3	43.2	56.8	5.3885	0.0089
Crystallin, mu	gi 56789444	98	34064	5.2	39500	5.3				
Tubulin alpha	gi 223556	71	52335	4.7	39500	5.3				
Similar to Beta-soluble NSF attachment protein (SNAP-beta) (N-ethylmaleimide-sensitive factor attachment protein, beta)	gi 34859344	120	40357	6.1	37000	5.3	60.5	39.5	7.8568	0.0070
Gamma-actin [Mus musculus]	gi 809561	73	42055	5.6	34000	5.5	55.0	45.0	2.7393	0.0013
Actin beta - rat	gi 71620	72	42786	5.2	34000	5.5				
Ubiquitin-conjugating enzyme E2N (homologous to yeast UBC13)	gi 58477429	105	17290	6.5	16000	5.7	59.7	40.3	5.0217	0.0009
Cytochrome c oxidase subunit Va preprotein	gi 55971	89	16828	6.5	15000	5.2	62.3	37.7	6.2369	0.0008
Cytochrome c oxidase, subunit Va [Mus musculus]	gi 21707954	89	16800	6.5	15000	5.2				
Malate dehydrogenase, mitochondrial	gi 42476181	185	37077	8.9	36000	7.6	62.7	37.3	5.0763	0.0002
Similar to hemoglobin alpha chain	gi 34870607	77	15806	8.5	15000	7.3	62.7	37.3	4.3678	<0.0001

Table S5
Juvenile versus senescent HUVEC (mitochondrial preparation)
All accession numbers are from Homo sapiens if not stated otherwise

Protein	Identification						Quantification			
	Accession Number	PMF score	Mass	pI	exp. Mass	exp. pI	Juv (%)	Sen (%)	StdDev (%)	p-value
Tubulin, beta 6	gi 14210536	203	51242	4.5	60333	4.933	55.6	44.4	7.4303	0.0024
Tubulin, beta polypeptide	gi 57209813	159	48976	4.4	60333	4.933				
Tubulin, beta, 2	gi 23958133	150	51225	4.6	60333	4.933				
Tubulin, beta polypeptide	gi 57209813	181	47736	4.4	63000	4.9	57.2	42.8	8.8069	0.0012
TUBB protein	gi 16198437	152	30340	4.5	63000	4.9				
Tubulin, beta 2	gi 4507729	146	49875	4.5	63000	4.9				
Protein disulfide isomerase-related protein 5	gi 1710248	167	46170	4.7	51333	5	64.4	35.6	8.6217	<0.0001
Calumenin precursor	gi 4502551	100	37084	4.2	48000	4.5	39.1	60.9	6.6477	<0.0001
Calumenin	gi 2809324	89	37404	4.2	48000	4.5				
Crocalbin-like protein	gi 8515718	79	34968	4.2	48000	4.5				
Reticulocalbin 3, EF-hand calcium binding domain	gi 28626510	164	37470	4.5	46500	4.6	33.8	66.2	8.6449	<0.0001
Reticulocabin precursor	gi 9963785	148	37401	4.5	46500	4.6				
RCN3 protein	gi 15488585	112	37470	4.5	46500	4.6				
Reticulocalbin 3, EF-hand calcium binding domain	gi 28626510	146	37470	4.5	47333	4.6	34.1	65.9	7.7465	<0.0001
RCN3 protein	gi 15488585	131	37470	4.5	47333	4.6				
Reticulocabin precursor	gi 9963785	130	37401	4.5	47333	4.6				
Reticulocalbin 3, EF-hand calcium binding domain	gi 28626510	238	37470	4.5	47000	4.633	35.1	64.9	7.1699	<0.0001
RCN3 protein	gi 15488585	189	37470	4.5	47000	4.633				
Reticulocabin precursor	gi 9963785	172	37401	4.5	47000	4.633				
Reticulocalbin 1, precursor	gi 14603330	231	38866	4.6	47000	4.667	32.1	67.9	5.6503	<0.0001
Reticulocalbin 1 precursor	gi 4506455	178	38866	4.6	47000	4.667				
Proliferation-inducing gene 20 protein	gi 41350407	128	19549	4.2	47000	4.667				
Reticulocalbin 1 precursor	gi 4506455	172	38866	4.6	47333	4.7	35.7	64.3	5.9005	<0.0001
Reticulocalbin 1, precursor	gi 14603330	154	38866	4.6	47333	4.7				
Reticulocalbin 3, EF-hand calcium binding domain	gi 28626510	118	37470	4.5	47333	4.7				
Reticulocalbin 1, precursor	gi 14603330	92	38866	4.6	46000	4.7	34.7	65.3	8.6589	<0.0001
Reticulocalbin 1 precursor	gi 4506455	108	38866	4.6	48000	4.75				
Vimentin	gi 62414289	103	53619	4.8	48000	4.75				
Proliferation-inducing gene 20 protein	gi 41350407	87	19549	4.2	48000	4.75	56.8	43.2	7.4033	0.0004
Laminin-binding protein	gi 34234	148	32128	4.6	45500	4.8				
Ribosomal protein SA	gi 31419811	147	33188	4.5	45500	4.8				
Chain A, 14-3-3 Protein Epsilon (Human) Complexed To Peptide	gi 67464424	120	26740	4.9	34666	4.6	52.9	47.1	4.2196	0.0046
Tyrosine 3/tryptophan 5 - monooxygenase activation protein, epsilon polypeptide	gi 5803225	117	29155	4.4	34666	4.6				
14-3-3 protein epsilon isoform transcript variant 1	gi 62131678	104	27018	4.8	34666	4.6				

Tropomyosin 4	gi 4507651	137	28504	4.4	31000	4.6	59.4	40.6	5.0676	<0.0001
Tropomyosin 4	gi 12803959	99	28907	4.4	31000	4.6				
TPM4-ALK fusion oncoprotein type 2	gi 10441386	98	27513	4.5	31000	4.6				
Unknown	gi 62822279	100	22142	4	26000	4.3	52.8	47.2	4.8803	0.0177
HIRA interacting protein 5 isoform 1	gi 50593025	99	25907	4.3	26000	4.3				
PREDICTED: similar to myosin:SUBUNIT=regulatory light chain isoform 2 [Pan troglodytes]	gi 114672411	79	17091	4.2	19000	4.5	65.7	34.3	7.8525	<0.0001
Human Complement Regulatory Protein Cd59 (Extracellular Region, Residues 1 - 70) (Nmr, Restrained Minimized Average Structure)	gi 515118	75	8081	6.9	19000	4.1	23.4	76.6	8.8621	<0.0001
Human Complement Regulatory Protein Cd59 (Extracellular Region, Residues 1 - 70) (Nmr, 10 Structures)	gi 515119	107	9851	6.9	18000	4.1	21.3	78.7	10.016	<0.0001
Cd59 Complexed With Glcnac-Beta-1,4-(Fuc-Alpha-1,6)- Glcnac-Beta-1 (Nmr, 10 Structures)	gi 640301	105	10726	5	18000	4.1				
Transmembrane protein 4	gi 7657176	100	21702	4.5	19000	4.8	63.9	36.1	6.0685	<0.0001
Human Complement Regulatory Protein Cd59 (Extracellular Region, Residues 1 - 70) (Nmr, 10 Structures)	gi 515119	105	9851	6.9	18000	4.1	16.3	83.7	14.212	<0.0001
Human Complement Regulatory Protein Cd59 (Extracellular Region, Residues 1 - 70) (Nmr, Restrained Minimized Average Structure)	gi 515118	112	8081	6.9	17333	4.5	66.4	33.6	7.037	<0.0001
Human Complement Regulatory Protein Cd59 (Extracellular Region, Residues 1 - 70) (Nmr, 10 Structures)	gi 515119	96	9851	6.9	17333	4.5				
CD59 antigen p18-20	gi 10835165	92	14168	6.5	17333	4.5				
Smooth muscle and non-muscle myosin alkali light chain, isoform 1	gi 16924329	231	17450	4.3	16000	4.433	56.6	43.4	6.4376	0.0001
Myosin, light polypeptide 6, alkali, smooth muscle and non-muscle, isoform 2	gi 62531190	217	17481	4.2	16000	4.433				
MYL6 protein	gi 113812151	120	15809	4.6	16000	4.433				
MYL6 protein	gi 113812151	118	15809	4.6	16000	4.5	53.6	46.4	6.9544	0.0284
Myosin, light chain 6, alkali, smooth muscle and non-muscle isoform 1	gi 17986258	117	16919	4.3	16000	4.5				
Motor protein	gi 516764	262	80191	5.8	158000	5.733	53.5	46.5	5.9509	0.0132
Transmembrane protein IMMT	gi 1160963	258	84856	6.4	158000	5.733				
	gi 48145703	246	83628	6.4	158000	5.733				
Heat shock 70kDa protein 9B (mortalin-2)	gi 12653415	116	73682	6.2	111666	5.4				

Chaperonin	gi 41399285	387	61548	5.5	99250	5.2	52.5	47.5	4.4749	0.0198
Heat shock protein 60	gi 77702086	377	61706	5.7	99250	5.2				
Chaperonin	gi 31542947	324	61016	5.5	99250	5.2				
Heat shock protein 60	gi 77702086	418	61706	5.7	95000	5.225	52.6	47.4	5.6461	0.0459
Chaperonin	gi 41399285	414	61548	5.5	95000	5.225				
Chaperonin	gi 31542947	316	61016	5.5	95000	5.225				
Chaperonin	gi 31542947	113	61016	5.5	93000	5.45	58.5	41.5	8.4936	0.0002
Heat shock protein 60	gi 77702086	113	61174	5.7	93000	5.45				
Protein disulfide isomerase-associated 3 precursor	gi 21361657	96	57986	6.3	93000	5.45				
T-complex protein 1 isoform a	gi 57863257	166	61899	6	106000	5.75	56.8	43.2	12.932	0.0248
T-complex polypeptide 1	gi 36796	166	61949	6.3	106000	5.75				
T-complex protein 1 isoform b	gi 57863259	143	44920	7.8	106000	5.75				
Vimentin	gi 37852	415	53830	4.8	85333	5.1	58.3	41.7	9.3182	0.0006
Vimentin variant	gi 62896523	397	53828	4.8	85333	5.1				
VIM	gi 47115317	290	53724	4.8	85333	5.1				
Unnamed protein product	gi 21748975	231	48428	5.4	91000	5.2	60.2	39.8	6.7373	<0.0001
G-rich RNA sequence binding factor 1	gi 53759145	231	49544	5.4	91000	5.2				
G-rich sequence factor-1	gi 517196	214	49563	5.5	91000	5.2				
unnamed protein product	gi 21748975	164	48428	5.4	79250	5.2	61.3	38.7	7.3964	<0.0001
G-rich RNA sequence binding factor 1	gi 53759145	164	49544	5.4	79250	5.2				
G-rich sequence factor 1 (GRSF-1)	gi 55977848	150	51732	5.8	79250	5.2				
Chain H, Human mitochondrial aldehyde dehydrogenase complexed with NAD ⁺ and Mn ²⁺	gi 6137684	167	55475	5.8	82500	5.5	40.0	60.0	8.5166	<0.0001
Chain A, Human mitochondrial aldehyde dehydrogenase complexed with NAD ⁺ and Mn ²⁺	gi 6137677	167	53881	5.8	82500	5.5				
Chain H, Cys302ser mutant of human mitochondrial aldehyde dehydrogenase complexed with NAD ⁺ and Mg ²⁺	gi 33357604	166	55811	5.8	82500	5.5				
Chain A, Human mitochondrial aldehyde dehydrogenase complexed with NAD ⁺ and Mn ²⁺	gi 6137677	327	53881	5.8	77500	5.75	34.2	65.8	8.458	<0.0001
Chain A, Cys302ser mutant of human mitochondrial aldehyde dehydrogenase complexed with NAD ⁺ and Mg ²⁺	gi 33357547	326	54394	5.8	77500	5.75				
Chain H, Human mitochondrial aldehyde dehydrogenase complexed with NAD ⁺ and Mn ²⁺	gi 6137684	276	55475	5.8	77500	5.75				
Chain A, Human mitochondrial aldehyde dehydrogenase complexed with NAD ⁺ and Mn ²⁺	gi 6137677	273	53881	5.8	82000	5.9	36.7	63.3	9.6807	<0.0001

Chain A, Cys302ser mutant of human mitochondrial aldehyde dehydrogenase complexed with NAD ⁺ and Mg ²⁺	gi 33357547	272	54394	5.8	82000	5.9				
Chain H, Human mitochondrial aldehyde dehydrogenase complexed with NAD ⁺ and Mn ²⁺	gi 6137684	193	55475	5.8	82000	5.9				
Chain A, Human mitochondrial aldehyde dehydrogenase complexed with NAD ⁺ and Mn ²⁺	gi 6137677	302	53881	5.8	77500	5.75	39.6	60.4	8.0352	<0.0001
Chain A, Cys302ser mutant of human mitochondrial aldehyde dehydrogenase complexed with NAD ⁺ and Mn ²⁺	gi 33357547	301	54394	5.8	77500	5.75				
Chain H, human mitochondrial aldehyde dehydrogenase complexed with NAD ⁺ and Mn ²⁺	gi 6137684	234	55475	5.8	77500	5.75				
Putative protein STRF8	gi 41152530	125	42802	5.6	71000	5.35	59.8	40.2	6.4415	<0.0001
Putative protein STRF8	gi 41152530	175	42802	5.6	61333	5	59.8	40.2	11.523	0.0009
Solute carrier family 25 (mitochondrial carrier); phosphate carrier), member 24	gi 55959506	289	54029	6.2	63666	5.733	40.0	60.0	5.7997	<0.0001
Solute carrier family 25 member 24, isoform 1	gi 46249805	277	54013	6.2	63666	5.733				
Calcium-binding transporter	gi 6841066	240	46676	5.1	63666	5.733				
ACTB protein	gi 15277503	133	41257	5.6	72000	5.1	62.9	37.1	12.049	<0.0001
Actin, beta	gi 14250401	118	42041	5.6	72000	5.1				
Actin, gamma 1	gi 54696574	117	42828	5.2	72000	5.1				
Follistatin-like 1, precursor	gi 12652619	204	38504	5.2	52333	5.2	46.5	53.5	6.2261	0.0191
Follistatin-like 1 precursor	gi 5901956	184	34963	5.2	52333	5.2				
Follistatin-like 1 [Bos taurus]	gi 62988316	170	34834	5.3	52333	5.2				
ACTB protein	gi 15277503	73	41257	5.6	58000	5.9	55.7	44.3	8.716	0.0074
Actin, beta	gi 14250401	72	42041	5.6	58000	5.9				
Actin, gamma 1	gi 54696574	71	42828	5.2	58000	5.9				
Similar to heme oxygenase-2 isoform 2 [Pan troglodytes]	gi 114660701	147	32816	5.7	40000	5.4	41.9	58.1	6.3795	<0.0001
HMOX2	gi 48145637	144	35992	5.1	40000	5.4				
Annexin A2	gi 18645167	124	38552	7.9	37000	5.4	45.8	54.2	5.7594	0.0032
Potassium channel tetramerisation domain containing 12	gi 15489330	78	36564	5.3	43500	5.3	43.9	56.1	6.9257	0.0007
ANXA2 protein	gi 73909156	78	40503	8.4	43500	5.3				
Annexin A2	gi 18645167	63	38552	7.9	43500	5.3				
Protein phosphatase 1, catalytic subunit, alpha [Canis familiaris]	gi 50978728	195	37504	6.3	45666	5.833	62.7	37.3	10.087	<0.0001
Protein phosphatase 1, catalytic subunit, alpha isoform 1	gi 4506003	192	37488	6.2	45666	5.833				
Protein phosphatase 1, catalytic subunit, alpha isoform 3	gi 56790945	162	41085	6.6	45666	5.833				

PREDICTED: similar to N-ethylmaleimide-sensitive factor attachment protein, alpha isoform 7 [Pan troglodytes]	gi 114678095	192	32179	5.4	42000	5.3	45.6	54.4	4.9095	0.0006
N-ethylmaleimide-sensitive factor attachment protein, alpha	gi 47933379	189	33211	5	42000	5.3				
N-ethylmaleimide-sensitive factor attachment protein, alpha	gi 54696006	167	34628	5	42000	5.3				
HSPC124	gi 6841470	156	36519	5.7	40500	5.8	30.6	69.4	10.659	<0.0001
Inorganic pyrophosphatase 2 isoform 1 precursor	gi 29171702	155	37896	7.5	40500	5.8				
Pyrophosphatase	gi 5931600	73	32604	7.2	40500	5.8				
HSPC124	gi 6841470	151	36519	5.7	40000	5.933	40.1	59.9	7.3374	<0.0001
Inorganic pyrophosphatase 2 isoform 1 precursor	gi 29171702	137	37896	7.5	40000	5.933				
PPA2 protein	gi 34980942	101	35875	8.6	40000	5.933				
Peroxisomal enoyl-coenzyme A hydratase-like protein	gi 70995211	163	35793	8.1	37333	5.933	31.6	68.4	11.699	<0.0001
Peroxisomal enoyl-coenzyme A hydratase-like protein	gi 15080016	150	36856	8.1	37333	5.933				
Enoyl Coenzyme A hydratase 1, peroxisomal	gi 16924265	146	35735	8.4	37333	5.933				
PREDICTED: similar to prohibitin isoform 4 [Macaca mulatta]	gi 109114264	219	28047	5.5	32250	5.3	43.2	56.8	9.8958	0.0049
PREDICTED: similar to prohibitin isoform 3 [Macaca mulatta]	gi 109114262	216	29074	5.4	32250	5.3				
Prohibitin	gi 46360168	204	29979	5.5	32250	5.3				
P2ECSL	gi 11275665	106	24298	5.7	32000	5.55	40.0	60.0	11.013	0.0005
Unnamed protein product	gi 28317	70	60200	4.9	32000	5.55				
Chloride intracellular channel 2	gi 66346733	163	28338	5.3	33500	5.4	29.1	70.9	13.388	<0.0001
PREDICTED: similar to Chloride intracellular channel 2 isoform 2 [Pan troglodytes]	gi 114690746	144	24360	5.8	33500	5.4				
PHB	gi 49456373	98	29991	5.5	33500	5.4				
DCI protein	gi 16307101	127	26965	6.8	32000	5.933	36.3	63.7	9.5303	<0.0001
Chain A, Crystal Structure Of Human Mitochondrial Delta3-Delta2- Enoyl-Coa Isomerase	gi 60593479	125	28571	6.3	32000	5.933				
Dodecenoyl-Coenzyme A delta isomerase (3,2 trans-enoyl-Coenzyme A isomerase)	gi 12653937	118	32779	8.7	32000	5.933				
PREDICTED: apolipoprotein A-I binding protein isoform 2 [Pan troglodytes]	gi 114560275	144	20418	7	31500	5.3	40.5	59.5	8.839	<0.0001
APOA1BP protein	gi 71681685	126	21126	7	31500	5.3				
Apolipoprotein A-I binding protein precursor	gi 91984773	124	31654	7.8	31500	5.3				
Chain B, Cathepsin B	gi 999909	127	22401	5	30500	5.1	22.1	77.9	14.079	<0.0001

(E.C.3.4.22.1)										
Cathepsin B	gi 741376	117	17143	5.5	30500	5.1				
Refined Crystal Structure Of Human Procathepsin B At 2.5 Angstrom Resolution	gi 2982152	75	37801	6.3	30500	5.1				
Peroxiredoxin 3	gi 14250063	60	27705	7.6	25000	5.6	44.6	55.4	4.8576	<0.0001
Peroxiredoxin 3 isoform b	gi 32483377	180	26708	7.5	27000	5.85	46.6	53.4	6.7102	0.0300
Peroxiredoxin 3, isoform a precursor	gi 14250063	178	28768	7.6	27000	5.85				
Peroxiredoxin 3 isoform a precursor variant	gi 62896877	166	28670	7.9	27000	5.85				
SPRY domain containing 4	gi 46409324	172	23084	7	22000	5.2	44.0	56.0	5.3599	<0.0001
Mitochondrial ribosomal protein L50	gi 21265096	153	18845	8.1	16500	5.875	52.0	48.0	3.7915	0.0285
Mitochondrial ribosomal protein L50	gi 21618939	81	18347	8.1	16500	5.875				
PREDICTED: glutaminase C isoform 3 [Pan troglodytes]	gi 114582297	169	67897	8.1	49500	4.7	33.0	67.0	19.735	0.0020
Glutaminase isoform C	gi 6002671	145	60239	6.5	49500	4.7				
Glutaminase C	gi 5690372	143	67909	8	49500	4.7				
Succinate dehydrogenase complex, subunit A, flavoprotein precursor	gi 4759080	122	75831	7.4	45333	4.133	34.8	65.2	16.511	0.0011
Succinate dehydrogenase complex, subunit A, flavoprotein precursor variant	gi 62087562	122	76317	7.3	45333	4.133				
Glutaminase isoform C	gi 6002671	73	60239	0	45333	4.133				
ATP synthase, H ⁺ transporting, mitochondrial F1 complex, alpha subunit, precursor	gi 24660110	285	61456	0	38000	4.533	40.2	59.8	11.233	0.0018
ATP synthase, H ⁺ transporting, mitochondrial F1 complex, alpha subunit precursor	gi 4757810	282	60068	0	38000	4.533				
ATP5A1 protein	gi 34782901	223	49119	9.5	38000	4.533				
Keratin, type I cytoskeletal 9 (Cytokeratin-9) (CK-9) (Keratin-9) (K9)	gi 81175178	113	62800	5	42000	4.85	39.8	60.2	14.312	0.0076
keratin 1	gi 17318569	110	66558	0	42000	4.85				
ATP5A1 protein	gi 34782901	82	49119	9.5	42000	4.85				
Chain A, Latent Form Of Plasminogen Activator Inhibitor-1 (Pai-1)	gi 10835819	132	42742	0	31666	4.433	58.4	41.6	11.957	0.0084
Chain A, Human Plasminogen Activator Inhibitor Type-1 In Complex With A Pentapeptide	gi 4699714	101	42800	7.2	31666	4.433				
Plasminogen activator inhibitor	gi 755747	83	43389	7.2	31666	4.433				
ACTB protein	gi 15277503	105	41257	5.6	22250	3.975	40.8	59.2	10.477	0.0017
ALDOA	gi 49456715	180	40840	8.4	28333	5.267	48.2	51.8	3.5515	0.0484
Flotillin	gi 6563242	62	28216	8.6	28333	5.267				
Annexin A2 (Annexin II) (Lipocortin II) (Calpactin I heavy chain) (Chromobindin-8) (p36) (Protein I) (Placental anticoagulant protein IV) (PAP-IV)	gi 113950	193	39288	0	18000	3.4	40.6	59.4	15.065	0.0168

Annexin A2	gi 18645167	193	39260	0	18000	3.4				
Chain A, Annexin A2: Does It Induce Membrane Aggregation By A New Multimeric State Of The Protein	gi 56966699	193	39346	0	18000	3.4				
Mitochondrial ribosomal protein S22	gi 9910244	109	41786	0	20000	3.1	55.6	44.4	9.0574	0.0175
VDAC2	gi 48146045	112	31810	7.2	16500	3.7	44.9	55.1	8.5338	0.0212
Voltage-dependent anion channel 2	gi 55664661	112	31923	7.9	16500	3.7				
Voltage-dependent anion channel VDAC2 - human	gi 346412	111	33168	7.7	16500	3.7				
Peroxisomal enoyl-coenzyme A hydratase-like protein	gi 70995211	76	36856	8.1	16250	3.25	38.7	61.3	11.703	0.0007
Enoyl Coenzyme A hydratase 1, peroxisomal	gi 16924265	76	36798	8.4	16250	3.25				
Endoplasmic reticulum protein 29, isoform 1 precursor	gi 75517652	127	29152	7.5	13500	3.3	41.0	59.0	13.563	0.0119
Dihydropteridine reductase (HDHPR) (Quinoid dihydropteridine reductase) Chain , Dihydropteridine Reductase (Dhpr) (E.C.1.6.99.7) Complexed With Nadh	gi 118600	68	26495	0	13500	3.3				
	gi 640447	68	26481	0	13500	3.3				
Unnamed protein product	gi 28071074	88	14065	9.7	28000	7.6	41.4	58.6	9.3998	0.0012
X-Ray Crystal Structure Of The Human Galectin-3 Carbohydrate Recognition Domain (Crd) At 2.1 Angstrom Resolution	gi 3402185	86	15750	9.9	28000	7.6				
Chain A, Crystal Structure Of The Human Galectin-3 Crd In Complex With A 3'-Derivative Of N-Acetylactosamine	gi 66360056	84	16518	9.4	28000	7.6				
Hydroxyacyl-Coenzyme A dehydrogenase, type II isoform 2	gi 83715985	101	26676	7.3	16666	4.967	45.6	54.4	7.0474	0.0177
Hydroxyacyl-Coenzyme A dehydrogenase, type II isoform 1	gi 4758504	99	27614	7.9	16666	4.967				
Endoplasmic reticulum-associated amyloid beta peptide-binding protein	gi 20336350	91	21099	8.1	16666	4.967				
RAB5C, member RAS oncogene family isoform b	gi 41393545	63	24176	0	12000	3.9	40.9	59.1	9.8391	0.0011
RAB5C, member RAS oncogene family isoform b	gi 41393545	101	24176	0	11500	4.1	38.8	61.2	9.8909	0.0002
Rab5c-like protein, similar to Canis familiaris Rab5c protein, PIR Accession Number S38625	gi 508285	99	24261	0	11500	4.1				
Superoxide dismutase [Mn], mitochondrial	gi 38503334	121	22549	7.3	10750	3.425	36.7	63.3	13.34	0.0006
Chain A, Human Manganese Superoxide Dismutase	gi 2780818	121	22530	7.4	10750	3.425				

Mutant Q143n										
Superoxide dismutase [Mn], mitochondrial	gi 38503339	121	22544	7.4	10750	3.425				
Fracture callus 1 homolog	gi 6912382	131	11579	7.5	15000	6.6	53.4	46.6	5.2589	0.0128
Cytochrome c oxidase subunit Vb precursor	gi 17017988	77	14395	9	8333	4.367	52.9	47.1	4.6937	0.0163
COX5B	gi 180937	77	14394	9.4	8333	4.367				
Thiopurine S-methyltransferase (Thiopurine methyltransferase)	gi 84029582	73	28100	6.4	8333	4.367				
Beta-myosin heavy chain	gi 601916	66	7885	10.1	13000	8	41.1	58.9	4.2402	<0.0001

Table S6
Juvenile versus tBHP-treated HUVEC (mitochondrial preparation)
All accession numbers are from Homo sapiens if not stated otherwise

Protein	Identification						Quantification			
	Accession Number	PMF score	Mass	pI	exp. Mass	exp. pI	Poolt BHP (%)	PoolY (%)	StdDev (%)	p-value
Tubulin, beta 6	gi 14210536	203	51242	4.5	60333	4.933	39.0	61.0	0.6173	0.0253
Tubulin, beta polypeptide	gi 57209813	159	48976	4.4	60333	4.933				
Tubulin, beta, 2	gi 23958133	150	51225	4.6	60333	4.933				
Tubulin, beta polypeptide	gi 57209813	181	47736	4.4	63000	4.9	33.0	67.0	1.5181	0.0402
TUBB protein	gi 16198437	152	30340	4.5	63000	4.9				
Tubulin, beta 2	gi 4507729	146	49875	4.5	63000	4.9				
Laminin-binding protein	gi 34234	148	32128	4.6	45500	4.8	40.5	59.5	0.6006	0.0284
Ribosomal protein SA	gi 31419811	147	33188	4.5	45500	4.8				
Corneal endothelium specific protein 1	gi 20069113	80	25551	4.1	39000	4.2				
Ovary-specific acidic protein	gi 12584947	77	28734	4.2	39000	4.2	34.7	65.3	0.3927	0.0116
Tropomyosin 4	gi 4507651	137	28504	4.4	31000	4.6				
Tropomyosin 4	gi 12803959	99	28907	4.4	31000	4.6				
TPM4-ALK fusion oncoprotein type 2	gi 10441386	98	27513	4.5	31000	4.6	37.7	62.3	0.3273	0.0119
Unknown	gi 62822279	100	22142	4	26000	4.3				
HIRA interacting protein 5 isoform 1	gi 50593025	99	25907	4.3	26000	4.3				
Motor protein	gi 516764	262	80191	5.8	158000	5.733	37.5	62.5	1.1014	0.0397
Transmembrane protein	gi 1160963	258	84856	6.4	158000	5.733				
IMMT	gi 48145703	246	83628	6.4	158000	5.733				
Heat shock protein 60	gi 77702086	418	61706	5.7	95000	5.225	36.0	64.0	0.341	0.0109
Chaperonin	gi 41399285	414	61548	5.5	95000	5.225				
Chaperonin	gi 31542947	316	61016	5.5	95000	5.225				
Alpha-tubulin	gi 37492	211	52251	4.8	74500	5.1	33.2	66.8	0.8983	0.0241
PREDICTED: similar to Tubulin alpha-6 chain (Alpha-tubulin 6) (Alpha-tubulin isotype M-alpha-6) isoform 1 [Canis familiaris]	gi 73996530	203	46042	5	74500	5.1				
PREDICTED: tubulin alpha 6 isoform 2 [Pan troglodytes]	gi 114644943	202	46028	5	74500	5.1				
Unnamed protein product	gi 21748975	231	48428	5.4	91000	5.2	32.2	67.8	1.4282	0.0362
G-rich RNA sequence binding factor 1	gi 53759145	231	49544	5.4	91000	5.2				
G-rich sequence factor-1	gi 517196	214	49563	5.5	91000	5.2				
Acyl-Coenzyme A dehydrogenase, short/branched chain, precursor	gi 15559225	179	48490	7	52000	5.733	39.0	61.0	0.6147	0.0251
Hypothetical protein	gi 30268183	164	47975	7.2	52000	5.733				
Acyl-Coenzyme A dehydrogenase, short/branched chain precursor	gi 4501859	159	47455	7	52000	5.733				
Glutathione peroxidase 1, isoform 1	gi 49522058	105	22960	6.5	29000	5.8	40.5	59.5	0.3182	0.0151

Glutathione peroxidase	gi 14717805	105	22818	6.5	29000	5.8					
Enolase 1	gi 4503571	121	48202	7.5	25000	3.3	39.2	60.8	0.7271	0.0304	
Enolase 1 variant	gi 62897945	121	48230	7.5	25000	3.3					
Enolase 1 variant	gi 62896593	121	48174	7.5	25000	3.3					
Citrate synthase precursor, isoform b	gi 38327627	107	45206	7.2	22750	3.65	35.8	64.2	1.2985	0.0411	
CS protein	gi 48257138	107	46118	7	22750	3.65					
Citrate synthase	gi 3288815	106	52559	8.2	22750	3.65					
ACTB protein	gi 15277503	65	41257	0	20750	3.475					
Chain A, Structure Of T255e, E376g Mutant Of Human Medium Chain Acyl-Coa Dehydrogenase PREDICTED: acyl-Coenzyme A dehydrogenase, C-4 to C-12 straight chain [Pan troglodytes]	gi 2392312	70	44678	0	22500	3.35	41.6	58.4	0.3814	0.0203	
Acyl-Coenzyme A dehydrogenase, C-4 to C-12 straight chain	gi 114557331	68	51915	0	22500	3.35					
Acyl-Coenzyme A dehydrogenase, C-4 to C-12 straight chain	gi 4557231	68	47975	0	22500	3.35					
Chain A, Human Mitochondrial Acetoacetyl-Coa Thiolase	gi 83755034	89	43347	7.8	21000	3.8	38.0	62.0	0.695	0.0260	
Mitochondrial ribosomal protein S22	gi 9910244	109	41786	0	20000	3.1	33.8	66.2	0.5715	0.0159	
Torsin A	gi 4557541	154	38847	7	17750	3.075	38.7	61.3	1.2518	0.0498	
Mitochondrial malate dehydrogenase 2, NAD	gi 89574129	259	33365	0	20600	5.04	37.4	62.6	0.6478	0.0231	
Unknown mitochondrial malate dehydrogenase precursor	gi 41472053	223	34624	0	20600	5.04					
	gi 21735621	219	36897	0	20600	5.04					
Porin 31HM [human, skeletal muscle membranes, Peptide, 282 aa]	gi 238427	235	30977	0	15250	3.925	34.2	65.8	0.1883	0.0054	
Voltage-dependent anion channel 1	gi 4507879	235	31108	0	15250	3.925					
2,4-dienoyl CoA reductase 1 precursor	gi 4503301	110	36930	0	15250	3.925					
Fracture callus 1 homolog	gi 6912382	131	11579	7.5	15000	6.6	37.9	62.1	0.2034	0.0076	

Table S7
Senescent versus tBHP-treated HUVEC (mitochondrial preparation)
All accession numbers are from Homo sapiens if not stated otherwise

Protein	Identification						Quantification			
	Accession Number	PMF score	Mass	pl	exp. Mass	exp. pl	Poolt BHP (%)	PoolSen (%)	StdDev (%)	p-value
Transmembrane protein 4	gi 7657176	100	21702	4.5	19000	4.8	67.8	32.2	1.0716	0.0271
Heat shock 70kDa protein 9B (mortalin-2)	gi 12653415	116	73682	6.2	111666	5.4	63.3	36.7	0.0847	0.0029
Unnamed protein product	gi 21748975	231	48428	5.4	91000	5.2	52.5	47.5	0.1305	0.0237
G-rich RNA sequence binding factor 1	gi 53759145	231	49544	5.4	91000	5.2				
G-rich sequence factor-1	gi 517196	214	49563	5.5	91000	5.2				
ACTB protein	gi 15277503	133	41257	5.6	72000	5.1	78.3	21.7	0.9677	0.0154
Actin, beta	gi 14250401	118	42041	5.6	72000	5.1				
Actin, gamma 1	gi 54696574	117	42828	5.2	72000	5.1				
ACTB protein	gi 15277503	73	41257	5.6	58000	5.9	69.3	30.7	0.3588	0.0084
Actin, beta	gi 14250401	72	42041	5.6	58000	5.9				
Actin, gamma 1	gi 54696574	71	42828	5.2	58000	5.9				
PREDICTED: apolipoprotein A-I binding protein isoform 2 [Pan troglodytes]	gi 114560275	144	20418	7	31500	5.3	41.9	58.1	0.7841	0.0437
APOA1BP protein	gi 71681685	126	21126	7	31500	5.3				
Apolipoprotein A-I binding protein precursor	gi 91984773	124	31654	7.8	31500	5.3				
NADH dehydrogenase-ubiquinone 30 kDa subunit	gi 10443631	372	30577	7.6	30000	5.475	42.7	57.3	0.4953	0.0305
NADH-Ubiquinone reductase	gi 5138999	372	30641	8.2	30000	5.475				
NADH dehydrogenase (ubiquinone) Fe-S protein 3, 30kDa (NADH-coenzyme Q reductase) variant	gi 62898071	292	30673	6.7	30000	5.475				
Chain A, Structure Of T255e, E376g Mutant Of Human Medium Chain Acyl-Coa Dehydrogenase	gi 2392312	70	44678	0	22500	3.35	34.8	65.2	0.3515	0.0104
PREDICTED: acyl-Coenzyme A dehydrogenase, C-4 to C-12 straight chain [Pan troglodytes]	gi 114557331	68	51915	0	22500	3.35				
Acyl-Coenzyme A dehydrogenase, C-4 to C-12 straight chain	gi 4557231	68	47975	0	22500	3.35				
VDAC2	gi 48146045	112	31810	7.2	16500	3.7	37.3	62.7	0.2604	0.0092
Voltage-dependent anion channel 2	gi 55664661	112	31923	7.9	16500	3.7				
Voltage-dependent anion channel VDAC2 - human	gi 346412	111	33168	7.7	16500	3.7				

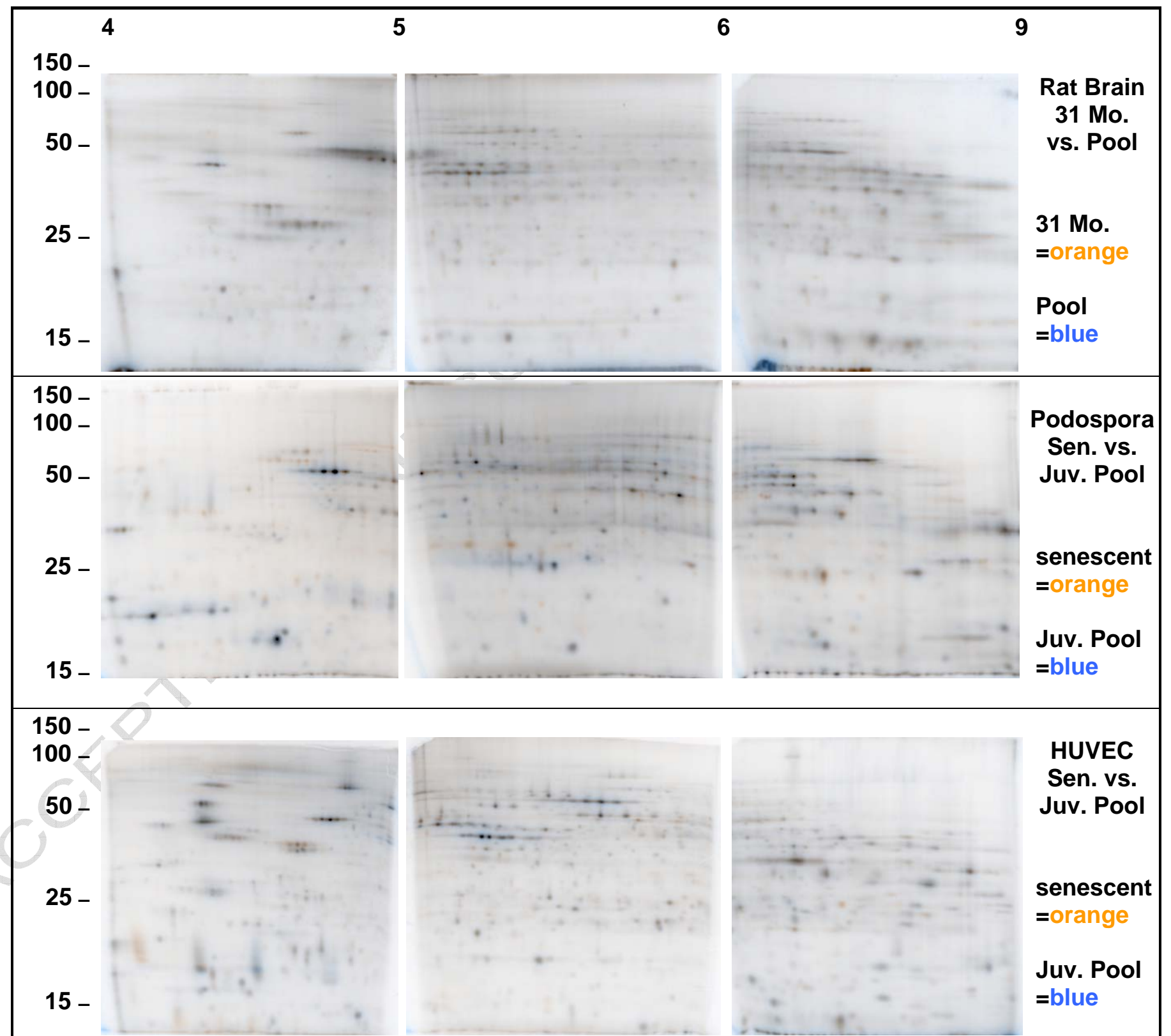


Figure 1

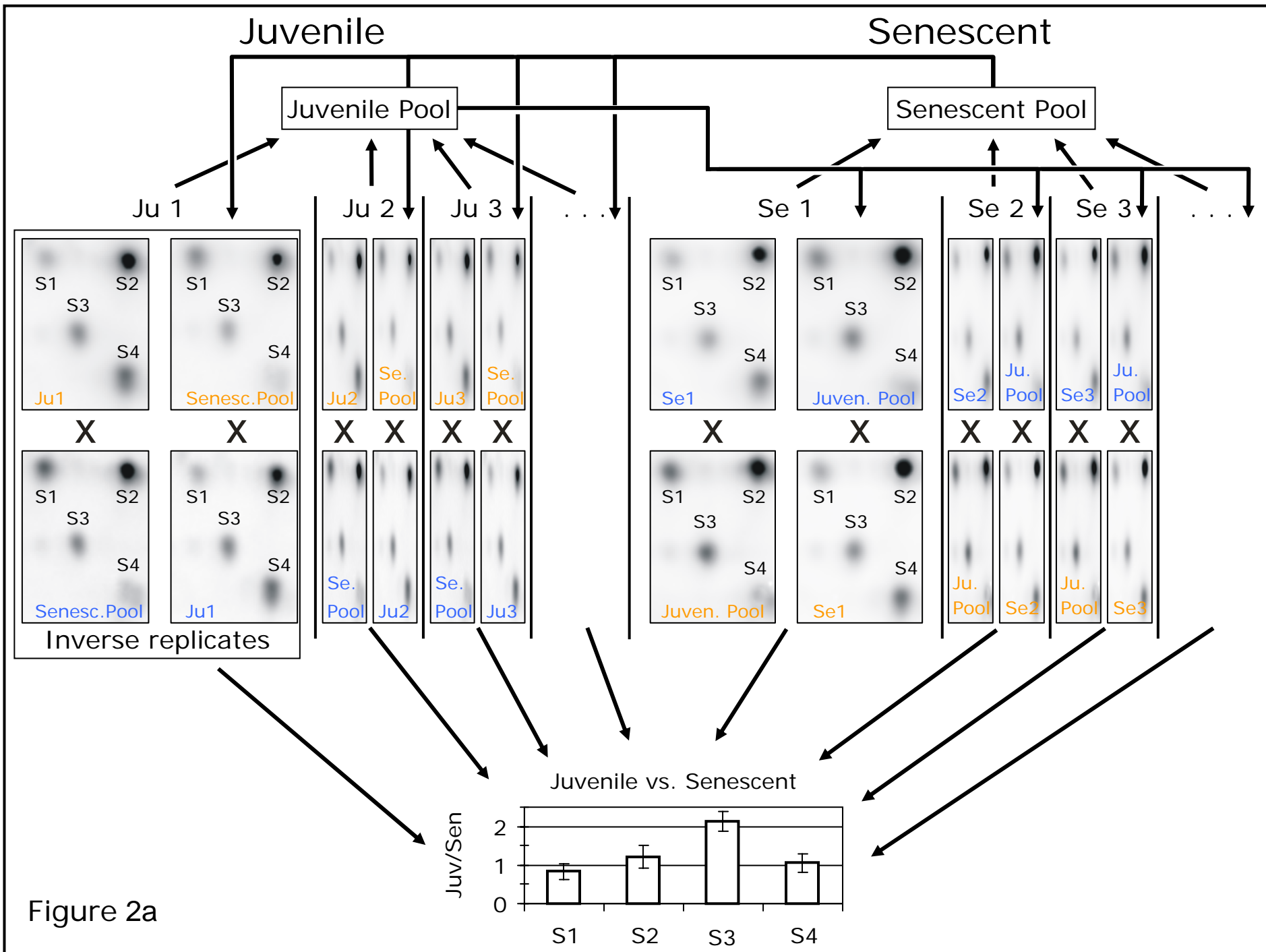


Figure 2a

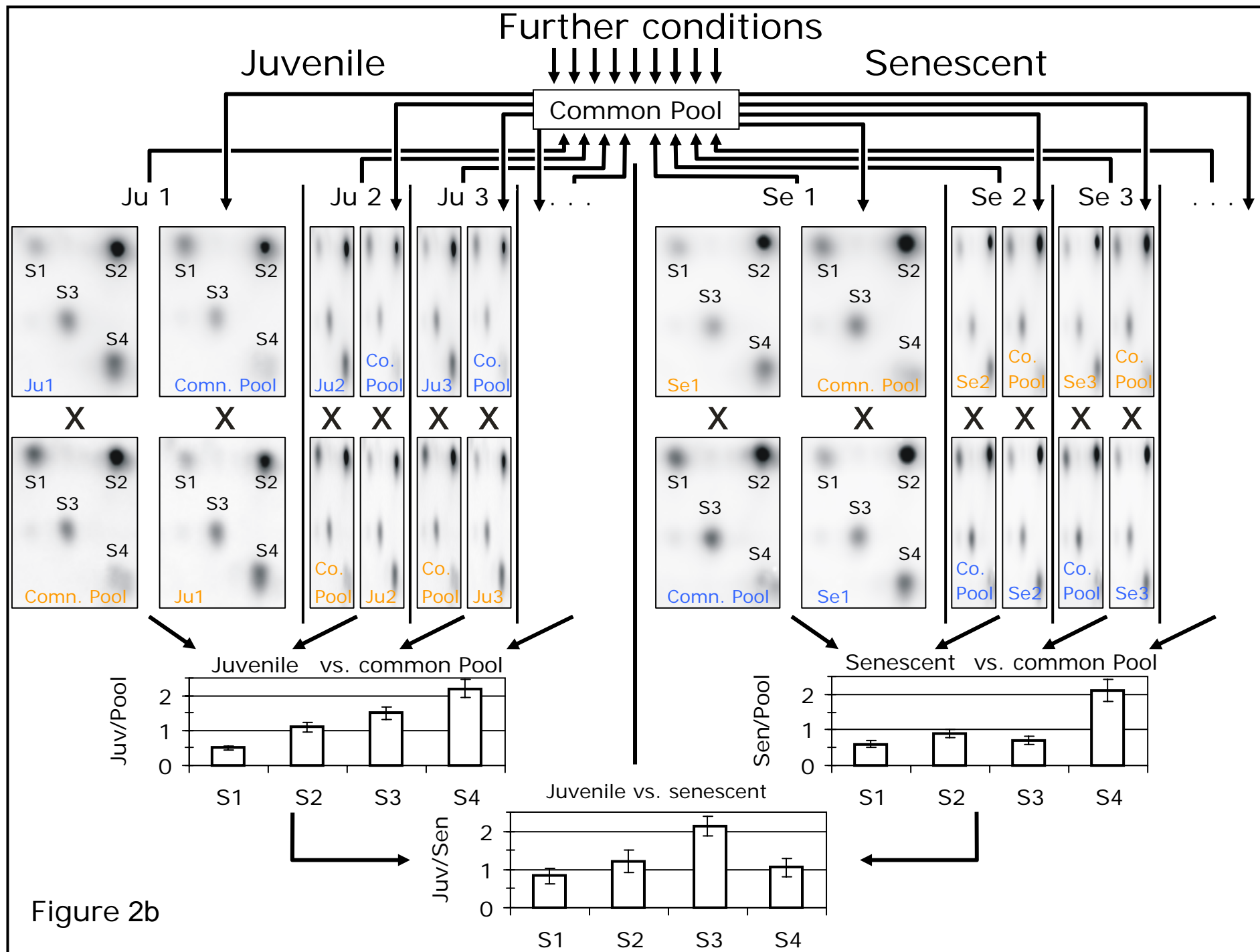
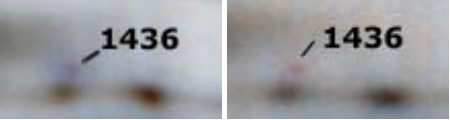

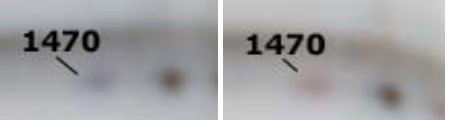
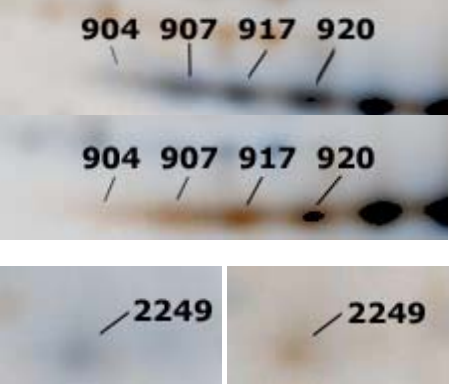

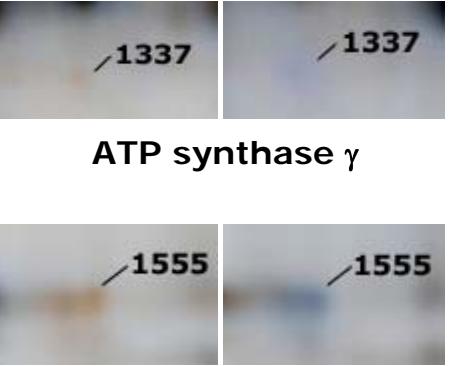
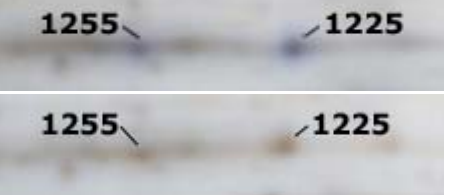


Figure 2b

pI range of gels, where ATP synthase subunit isoforms were found

4-5	5-6	6-9	
 <p>1436 1436</p> <p>ATP synthase β</p>	 <p>1685 1685</p> <p>1694 1694</p> <p>ATP synthase β</p>	 <p>1470 1470</p> <p>ATP synthase β</p>	<p>Rat Brain 31 Mo. vs. Pool</p>
 <p>904 907 917 920</p> <p>904 907 917 920</p> <p>2249 2249</p> <p>ATP synthase β</p>	 <p>1192 1192</p> <p>ATP synthase subunit 4</p>	 <p>1337 1337</p> <p>ATP synthase γ</p> <p>1555 1555</p> <p>ATP synthase OSC protein</p>	<p>Podospora Sen. vs. Juv. Pool</p>
		 <p>1255 1225</p> <p>1255 1225</p> <p>ATP synthase α</p>	<p>HUVEC Sen. vs. Juv. Pool</p>

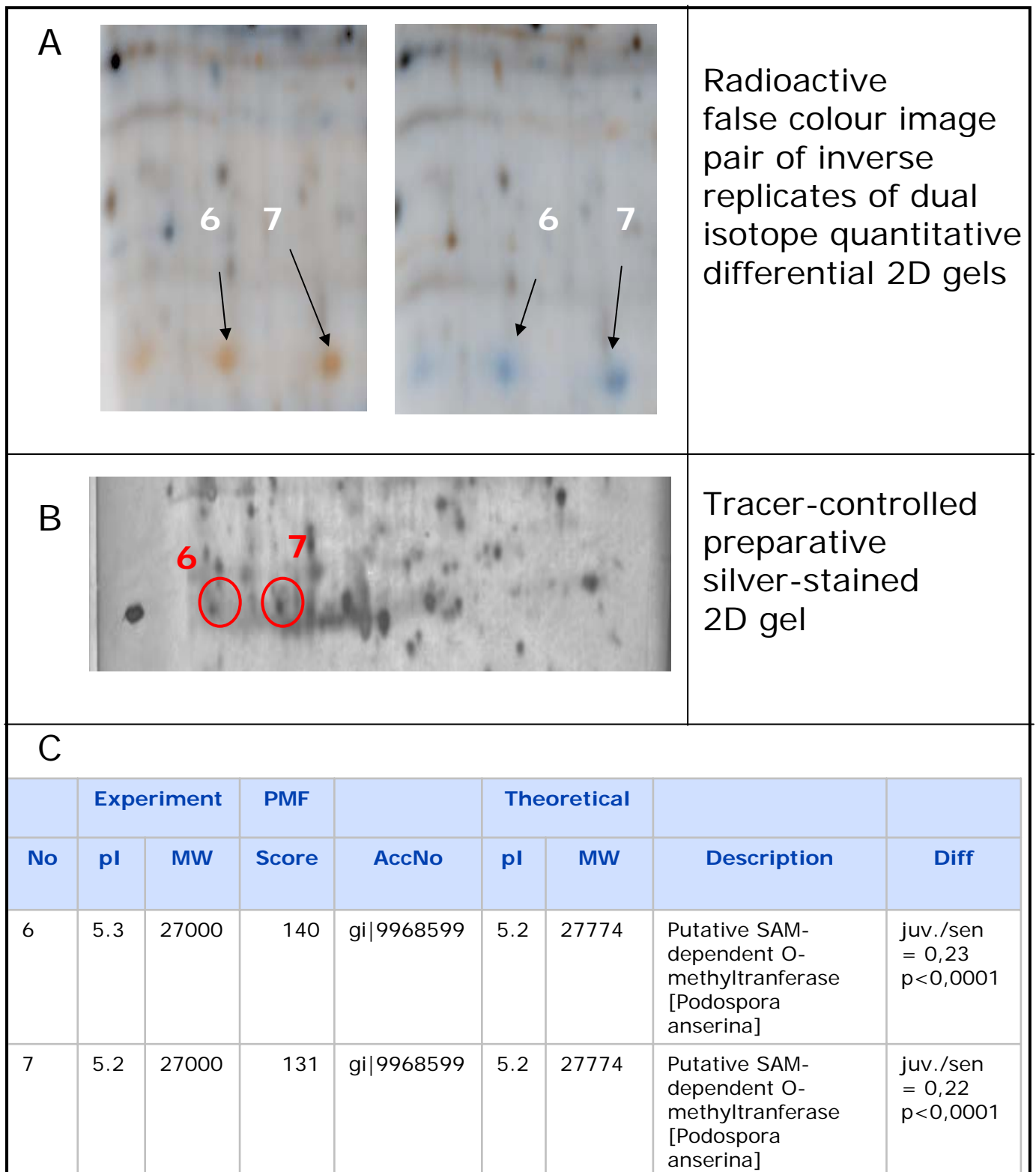


Figure 4